Design and Performance Evaluation of a Terahertz Metamaterial Biosensor for Tuberculosis Detection

A PROJECT REPORT

Submitted in Partial Fulfilment of the Requirements for the
Awards of the Degree
Of

Master of Science
in
Physics

Submitted by

BARBIE

24/MSCPHY/43

Under the supervision of

Dr. Ajeet Kumar

Associate Professor



Department of Applied Physics
Delhi Technological University
(Formerly Delhi College of Engineering)
Bawana Road, Delhi – 110042

May, 2026

DEPARTMENT OF APPLIED PHYSICS

DELHI TECHNOLOGICAL UNIVERSITY

(Formerly Delhi College of Engineering)

Bawana Road, Delhi – 110042

CANDIDATE'S DECLARATION

I, **Barbie (24/MSCPHY/43)**, hereby certify that the work which is being presented in the thesis entitled **"Design and Performance Evaluation of a Terahertz Metamaterial Biosensor for Tuberculosis Detection"** in partial fulfilment of the requirements for the Degree of Master of Science, submitted to the Department of Applied Physics, Delhi Technological University, is an authentic record of my own work carried out during the period from July 2025 to May 2026 under the supervision of Dr. Ajeet Kumar.

The matter presented in this thesis has not been submitted by me for the award of any other degree of this or any other University. The work has been communicated in SCI expanded with the following details:

Title of the paper: Design and Computational Analysis of High-Performance Terahertz - Inspired Metamaterial Biosensor for Tuberculosis Detection
Author names: Barbie, Pratibha Kumari, Deepak Garg and Ajeet Kumar
Name of journal: Journal of Electronic Materials
Status of the paper: Communicated
Date of paper communication: 2 April 2026
Date of paper acceptance: NA
Date of paper publication: NA

Place: Delhi **Barbie**

Date: 29th May 2026 (24/MSCPHY/43)

DEPARTMENT OF APPLIED PHYSICS

DELHI TECHNOLOGICAL UNIVERSITY

(Formerly Delhi College of Engineering)

Bawana Road, Delhi – 110042

SUPERVISOR CERTIFICATE

I hereby certify that the Project Dissertation titled **"Design and Performance Evaluation of a Terahertz Metamaterial Biosensor for Tuberculosis Detection"** which is submitted by **Barbie**, Roll No. **24/MSCPHY/43**, Department of Applied Physics, Delhi Technological University, Delhi in partial fulfilment of the requirement for the award of the Degree of **Master of Science**, is a record of the project work carried out by the student during the period from July 2025 to May 2026 under my supervision. To the best of my knowledge, this work has not been submitted in part or in full for any Degree or Diploma to this University or elsewhere.

Place: Delhi

Date: 29th May 2026

Dr. Ajeet Kumar

(Supervisor)

ACKNOWLEDGEMENT

I want to extend my heartfelt gratitude to my esteemed Supervisor, Dr. Ajeet Kumar, whose unwavering support, insightful guidance and invaluable mentorship has been instrumental at every stage of this research work on the applications of Metamaterials. His expert advice has been invaluable in shaping the direction and success of this work. My deepest thanks to Prof. Vinod Singh, Head, Department of Applied Physics, for providing the essential facilities and a conducive environment for our research.

I am also deeply thankful to the committee members for their valuable input and suggestions, which have enhanced the quality of my research work. I gratefully acknowledge Delhi Technological University for offering me the opportunity to conduct this research and for the extensive resources and support provided.

A special note of thanks to Mr. Deepak Garg, Ms. Pratibha Malik, a PhD scholar, for their constant motivation and invaluable assistance. Their encouragement and help have been a great source of inspiration throughout my research journey.

Lastly, my heartfelt gratitude to my family and friends. Their unwavering love and support have been my constant source of strength and motivation throughout this journey.

Barbie

(24/MSCPHY/43)

ABSTRACT

For the label-free and non-invasive detection of Tuberculosis (TB) cells, this work presents a detailed computational study of a highly sensitive Terahertz (THz) metamaterial (MM) based biosensor. The proposed structure are simulated and analyzed using CST Studio Suite. The finite element method (FEM) along with a frequency-domain electromagnetic (EM) solver are used to evaluate its performance characteristics. The proposed unit cell is consists of a ground plane made up of gold, an inexpensive dielectric substrate which is made up of paper material, and a top resonator which consists of two brick-shaped structure along with three closed circular ring structures placed between them. This resonator structure is made up of Vanadium dioxide (VO_2). The absorptivity curves are also evaluated by varying several geometrical parameters, such as the substrate thickness, the separation between the two bricks, and the radii of the rings etc. The optimized design achieves 99.88 % absorption at a resonance frequency of 3.3777 THz.

The sensing mechanism of the proposed sensor relies on the strong localization of electric and magnetic fields within the analyte layer at resonance. Consequently, small variations in the optical properties of the analyte sample, especially changes in the refractive index, can be accurately detected. A noticeable redshift in the resonant frequency is observed with the increase in the refractive index of the analyte, indicating a high sensitivity of the sensor to variations in the surrounding dielectric environment and enabling effective detection of TB cells. The proposed sensor exhibits clear resonance frequency variations in response to changes in the analyte, achieving a maximum sensitivity of 700 GHz/RIU for TB1. In addition, the highest quality factor (Q-factor) and figure of merit (FOM) values obtained are 16.2633 for TB4 and 3.4516 RIU^{-1} for TB1, respectively. These results indicate that the developed design has strong potential to be utilized as an effective computational platform for future development, fabrication, and experimental assessment of THz biosensors.

TABLE OF CONTENTS

Candidate's Declaration ii

Supervisor's Certificate iii

Acknowledgement iv

Abstract v

Table of Contents vi ,vii

List of Figures viii, ix

List of Tables x

List of Abbreviations xi

CHAPTER 1- Introduction 1-13

1.1 Classification of materials

1.2 Concept of Metamaterial

1.3 Some unusual properties of Metamaterials

1.4 Absorption Mechanism

1.4.1 Magnetic and Electrical Responses

1.4.2 Impedance Matching

1.4.3 Reduction in Plasma frequency

1.5 Applications of Metamaterial

1.6 Identified Research gaps and Challenges

1.6.1 Research Gaps

1.6.2 Challenges

CHAPTER 2- Research Objectives 14

CHAPTER 3- Literature Review 15-17

CHAPTER 4- Simulation Software 18-20

4.1 CST Studio Suite

4.2 Numerical Approach used in CST Studio Suite

CHAPTER 5- Numerical Analysis 21-24

5.1 Introduction

5.2 Mathematical Modelling

CHAPTER 6- Design and Methodology 25-33

6.1 Description of unit cell and Periodic Boundary conditions

6.2 Choice of materials

6.3 Methodology of Design

6.4 CST Simulation setup parameters (mesh type, ports, monitors)

CHAPTER 7- Parametric Optimization and Analysis 34-37

CHAPTER 8- Electromagnetic Field Distribution 38-41

CHAPTER 9- Results and Discussion 42-49

9.1 Evaluation of Refractive index sensor

9.2 Simulation Results and Analysis for Tuberculosis Detection

CHAPTER 10- Conclusion 50-51

CHAPTER 11- Future Perspectives 52

CHAPTER 12- References 53-59

LIST OF FIGURES

Fig.no.	Title of Figure	Page no.
1	Wave propagation in **(A)** RHM and **(B)** LHM.	2
2	Classification of materials	2
3	Meta atom as a building block of metamaterial	4
4	Conceptual Diagram of the Negative Refractive Index in Metamaterials	5
5	Phenomenon of invisibility cloaking	6
6	Showing phenomenon of inverse doppler effect	7
7	Showing mechanism of impedance matching in a metamaterial absorber	9
8	Various applications of Metamaterial	11
9	Computer Simulation Technology Logo	19
10	**(a)** Layout of 3×3 unit cell array of the proposed THz biosensor **(b)** Three-dimension schematic diagrams of the unit cell **(c)** The structural configuration and the front view of unit cell	26
11	Simulation model demonstrating the use of **(a)** periodic boundaries and **(b)** Floquet port settings applied in proposed unit cell	27
12	Design generation of proposed unit cell	29
13	Enhancement of the proposed absorber and response characteristics at various stages of absorber development **(a)** Reflection response and **(b)** Absorption characteristics.	31
14	**(a)** Showing mesh view of the proposed metamaterial biosensor **(b)** Port setup used for electromagnetic wave excitation **(c)** Frequency monitor setup for various analysis	32,33
15	Geometric parameter : Variation in substrate thickness	34
16	Geometric parameter: Variation in resonator thickness	35

17	Geometric parameter: Variation in inner radius of circular	36
18	Geometric parameter: Variation in half gap between bricks	37
19	Real |H|-field distribution at: **(a)** 3.3414 THz **(b)** 3.3777 THz (Resonance Frequency) **(c)** 3.4658 THz	39
20	Real |E|-field distribution at: **(a)** 3.3414 THz **(b)** 3.3777 THz (Resonance Frequency) **(c)** 3.4658 THz	40
21	Absorption characteristics of the proposed metamaterial unit cell	41
22	**(a)** Spectra of absorption for various refractive index **(b)** Linear fitting curve between resonant frequency and refractive index	44
23	Absorption characteristics of the proposed biosensor for tuberculosis (TB) detection: **(a)** TB1 **(b)** TB2 **(c)** TB3 **(d)** TB4	47

LIST OF TABLES

Table no.	Title of the Table	Page no.
1	Optimized parameter for the proposed Design	37
2	Various resonant frequencies (in THz) corresponding to the refractive index values.	43
3	The refractive index (RI) of normal and infected cell of TB	45
4	Performance of the proposed biosensor for Tuberculosis (Blood Sample) types corresponding normal cells	48
5	Sensitivity comparison between our design and existing metamaterial biosensor	49

LIST OF ABBREVIATIONS

Abbreviation	Full Form
TB	Tuberculosis
THz	Terahertz
MM	Metamaterial
FEM	Finite element method
EM	Electromagnetic
VO_2	Vanadium dioxide
RHM	Right- handed materials
LHM	Left - handed materials
DPS	Double positive materials
ENG	Epsilon negative materials
MNG	Mu negative materials
DNG	Double negative materials
SRR_S	Split – ring resonators
$CSRR_S$	Complementary split ring resonators
FOM	Figure of merit
Q-factor	Quality factor
RI	Refractive index
A	Absorption Capability
GHz	Gigahertz
S	Sensitivity
FWHM	Full width at half maximum
CST	Computer Simulation Technology
3D	Three dimensional

CHAPTER 1

INTRODUCTION

1.1 Classification of materials

The propagation behavior of electromagnetic waves in a material is strongly influenced by two important parameters: electric permittivity (ε) and magnetic permeability (μ). In conventional materials, where both of these parameters possess positive values, the electromagnetic wave follows the right-hand rule. In such media, the wave vector $\vec{k}$, which represents the direction of wave propagation, and the poynting vector $\vec{p}$, which indicates the direction of energy flow between the source (A) and receiver (B), point in the same direction. Materials exhibiting this behavior are commonly referred to as right-handed materials (RHM).

However, under certain conditions, both permittivity and permeability can attain negative values. In this case, the propagation characteristics of the electromagnetic wave become entirely different from those observed in conventional materials. The direction of energy flow and the direction of wave propagation become opposite to each other, meaning that the poynting vector $\vec{p}$ and wave vector $\vec{k}$, are oriented in reverse directions, as illustrated in fig.1. Materials showing this unusual electromagnetic behavior are known as left-handed materials (LHM), and they form the basis for many unique metamaterial properties such as negative refraction and reverse wave propagation [1-4].

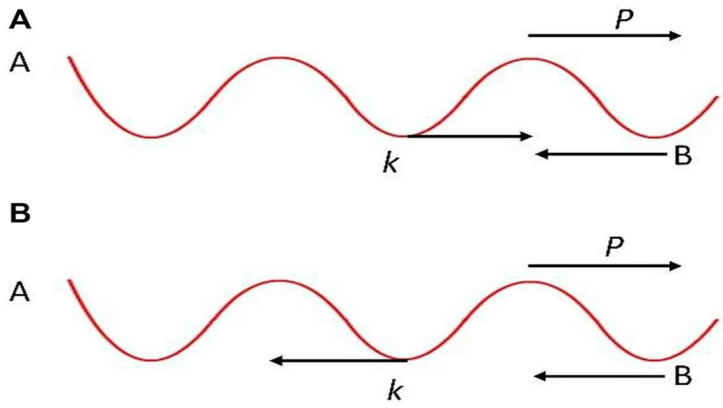


Fig.1 Wave propagation in **(A)** RHM and **(B)** LHM

Therefore, the propagation behavior of electromagnetic waves within a medium is mainly determined by the values of permittivity (ε) and permeability (μ). Based on the different combinations of these two parameters, materials can generally be classified into four distinct categories, as illustrated in fig.2.

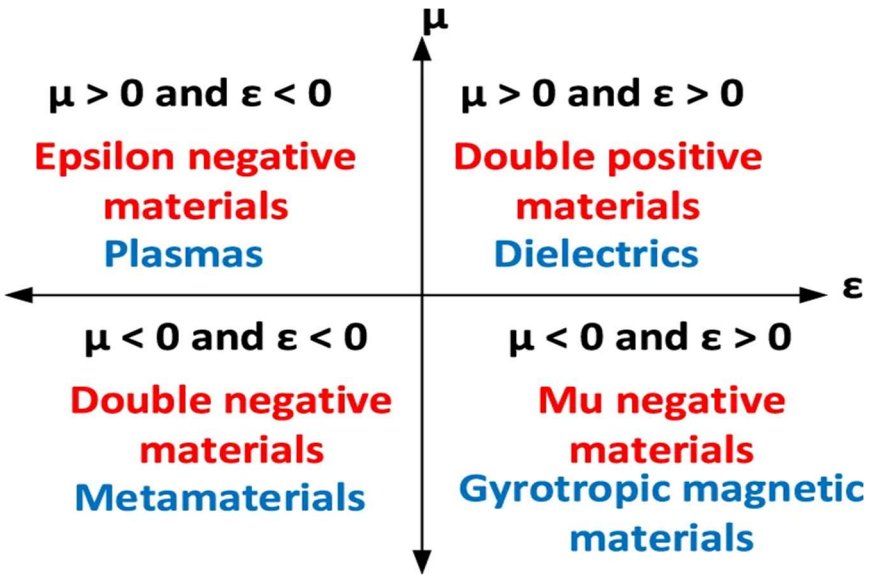


Fig.2 Classification of materials

Materials can be broadly classified into four categories based on the signs of their electric permittivity (ε) and magnetic permeability (μ). The first category is known as **double positive (DPS) materials**, in which both permittivity and permeability have positive values. Most naturally occurring dielectric materials belong to this group and exhibit normal electromagnetic wave propagation behavior.

The second category consists of **epsilon negative (ENG) materials**, where the permittivity becomes negative while the permeability remains positive. Certain plasma materials show this type of electromagnetic response within specific frequency ranges. Due to their negative permittivity characteristics, these materials interact with electromagnetic waves differently from conventional dielectrics.

The third category includes **mu negative (MNG) materials**, which possess positive permittivity and negative permeability. Materials with gyrotropic magnetic properties commonly exhibit this behaviour and have unique magnetic responses when exposed to electromagnetic fields.

The fourth category is referred to as **double negative (DNG) materials**, where both permittivity and permeability are negative simultaneously. These materials do not naturally exist but are artificially engineered using various metamaterial structures. One of the most unusual characteristics of these materials is that electromagnetic (EM) waves propagate in the reverse direction after entering the medium which results in negative refraction.

1.2 Concept of Metamaterial

Metamaterials are specially engineered materials that are designed to control and manipulate electromagnetic waves in ways that are not normally possible with naturally available materials. Unlike conventional materials, the behavior of metamaterials is largely governed by their structural design, size, geometry and arrangement of unit cells. These unique features allow metamaterials to exhibit unusual characteristics such as negative refractive index [5,6], near-perfect absorption [7,8], wave bending, cloaking effects [9], and polarization conversion [10,11].

The word metamaterial is came up from word meta which means beyond. This name reflects the extraordinary properties of these materials that are not found in conventional materials. The metamaterials was first introduced by Victor Veselago in 1968. He proposed that materials having both negative permittivity, permeability could show a negative refractive index. After major developments in fabrication technologies, microelectronics, and nanotechnology the practical implementation of such structures became achievable.

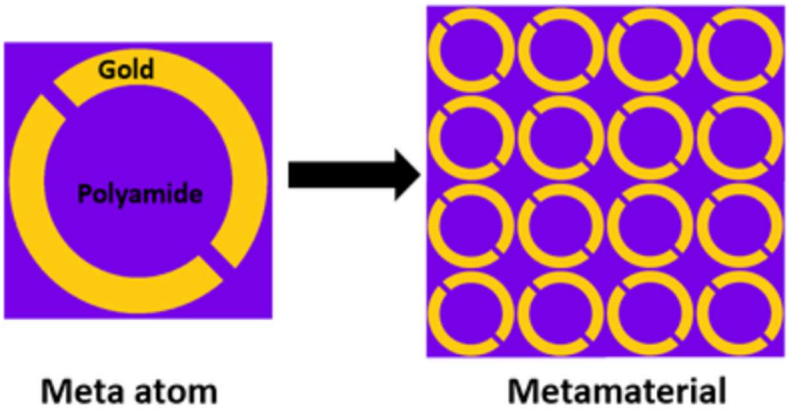


Fig.3 Meta atom as a building block of metamaterial

Metamaterials are generally formed by arranging artificially designed elements in a periodic manner, called as unit cells or meta-atoms [12-15]. These unit cells are usually much smaller than the wavelength of the incident electromagnetic wave, which results in phenomenon of effective homogeneous medium [16]. Different types of resonator geometries such as split-ring resonators (SRRs) [17], complementary split-ring resonators (CSRRs), circular rings, wire structures, and various patterned metallic elements are commonly used in metamaterial design. According to the specific application requirements, researchers modifying the structure and geometry of these metamaterial across various frequency ranges like in microwave, terahertz, infrared and optical [5].

1.3 Some Unusual Properties of Metamaterials

Metamaterials exhibit various unique properties that are generally not found in naturally occuring materials. These exceptional characteristics arise due to their structures rather than their chemical composition. By carefully designing the geometry, arrangement, and dimensions of the resonating elements, metamaterials can interact with electromagnetic waves in various unusual ways. Some of the major unusual properties of metamaterials are listed in this section.

1. Negative Refractive Index

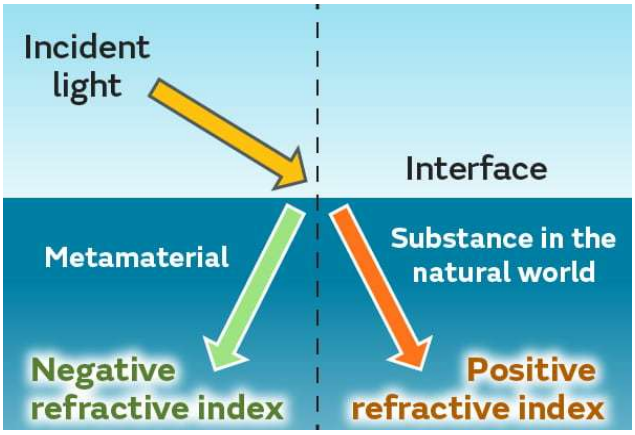


Fig.4 Conceptual Diagram of the Negative Refractive Index in Metamaterials

One of the most common features of metamaterials is their ability to produce a negative refractive index. In ordinary materials, electromagnetic waves bend in the usual direction when moving from one medium to another but in metamaterials which have both negative electric permittivity (ε) and magnetic permeability (μ) cause electromagnetic waves to refract in the opposite direction.

$$n = \sqrt{\varepsilon\mu} \qquad (1)$$

This unusual behavior of metamaterial is known as negative refraction.

2. Near-Perfect Electromagnetic Absorption

Metamaterials can be designed to absorb incident electromagnetic waves almost completely which can be done by carefully optimizing the resonator geometry and impedance matching conditions, which results into minimise reflection and transmission also allowing the incoming energy to be trapped inside the structure.

3. Electromagnetic Cloaking Capability

Another extraordinary property of metamaterials is their potential to achieve electromagnetic cloaking. In such structures, electromagnetic waves can be guided around an object in a controlled manner, reducing scattering and making the object partially invisible to detection systems. This phenomenon is mainly based on transformation optics and gradient-index metamaterial designs.

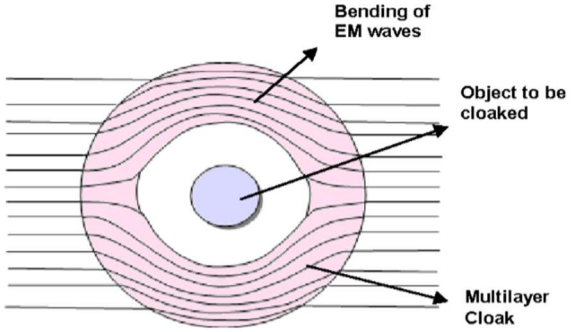


Fig.5 Phenomenon of invisibility cloaking

4. Super-Lensing and Subwavelength Imaging

Traditional optical lenses are restricted by the diffraction limit, which limits the resolution of imaging systems. Metamaterials can overcome this limitation by amplifying evanescent waves and focusing electromagnetic energy at dimensions smaller than the wavelength. As a result, metamaterial-based super-lenses can generate extremely high-resolution images.

5. Strong Localization of Electromagnetic Fields

Metamaterials are capable of producing highly concentrated electric and magnetic fields around their resonating structures. Due to resonance effects, electromagnetic energy becomes confined within a very small region, leading to enhanced wave–matter interaction. This strong field localization improves the performance of biosensors, chemical sensors, nonlinear optical devices, and energy harvesting systems.

6. Reverse Doppler Effect

Metamaterials may also demonstrate the reverse Doppler effect, which behaves opposite to the conventional Doppler phenomenon. Normally, when a source approaches an observer, the observed frequency increases. However, in metamaterials with negative refractive index, the frequency shift occurs in the reverse manner.

This effect has importance in communication systems, wave physics, and signal processing technologies.

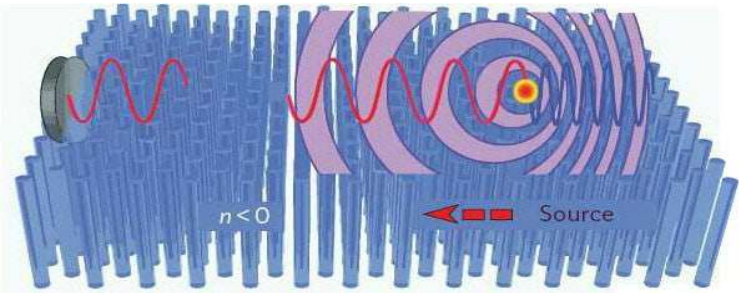


Fig. 6 Showing phenomenon of inverse doppler effect

1.4 Absorption Mechanism

These structures show absorption behaviour because of several significant factors, like negative values of electric permittivity (ε) and magnetic permeability (μ), effective impedance matching to free space, reduction of the metal plasma frequency, and excitation of strong electric and magnetic responses. The geometry of the absorber can be carefully designed and optimized to control and improve the overall absorption performance. The interaction between the electromagnetic waves and the structure can be effectively studied by altering the shape, size and arrangement of the resonating elements. The three main absorption mechanisms are discussed in more detail in the following subsections.

1.4.1 Magnetic and Electrical Responses

The absorption behavior is mainly governed by the combined effects of electric and magnetic resonances generated within the structure. Magnetic resonance is produced through loop-shaped or closed-ring geometries, while electric resonance is commonly produced by introducing gaps or splits in the resonating elements. By carefully optimizing the geometry and arrangement of these structures, both the electric and magnetic responses can be effectively controlled and changed according to the desired operating frequency requirement. Among the various resonator configurations, the split ring resonator (SRR) is one of the most commonly used designs in metamaterial absorbers. SRR-based structures are widely preferred because they support both magnetic and electric resonances which enables strong electromagnetic absorption characteristics.

The interaction between these absorber structures generate additional absorption resonances, while the arrangement of closely positioned concentric split-ring resonators (SRRs) generate broad absorption bandwidth characteristics.

1.4.2 Impedance Matching

Another important mechanism responsible for electromagnetic (EM) wave absorption is impedance matching. When electromagnetic waves propagate from one medium into another, causing a portion of the incident energy to be reflected while the remaining energy is transmitted through the material then this phenomenon occurs. The amount of reflection becomes minimum when the characteristic impedance of the absorbing structure closely matches the impedance of the incident medium, as shown in fig.7. Therefore, achieving proper impedance matching is considered one of the most critical and challenging point in the design of perfect absorbers.

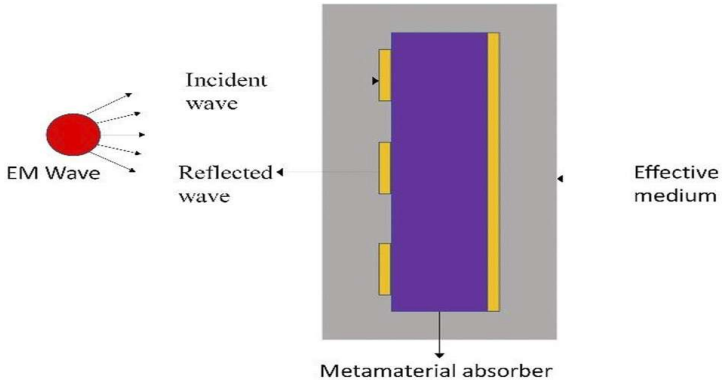


Fig.7 Showing mechanism of impedance matching in a metamaterial absorber

1.4.3 Reduction in Plasma Frequency

The plasma frequency of a material is the frequency at which the free electron cloud in the material naturally oscillates and it can be written as:

$$w_p = \sqrt{\frac{Ne^2}{m\varepsilon_o}}\, w_p \qquad (2)$$

where,

- w_p is plasma frequency
- N is density of the free electron gas
- m is effective mass
- e is charge of an electron

Equation 2 clearly indicates that the plasma frequency w_p is dependent on the concentration of free electron carriers present within the metal as the plasma frequency and carrier concentration are directly proportional. By increasing or decreasing the doping concentration, the electrical properties of the material can be modified accordingly. In metamaterial absorbers, negative permittivity can be achieved by lowering the plasma frequency in relation to the desired operating frequency range. The primary objective behind reducing the plasma frequency is to enable metamaterial absorbers to function effectively across different frequency regions. Hence, it becomes essential to carefully tune the plasma frequency so that it matches the intended operating frequency regime of the absorber [18-20].

1.5 Applications of Metamaterial

Metamaterials have a wide range of possible uses, such as optical filtering, biomedical sensing [21], aerospace systems, sensors, and structural monitoring.

They are also explored for telecommunications [22-24], optics [25-27], sensing and image processing [28-31] and energy harvesting [32, 33]. Research is further looking at improving ultrasonic sensing, earthquake-resistant structures, and even creating super-lenses or limited forms of invisibility using gradient-index designs. Acoustic and seismic metamaterials continue to be active research topics.

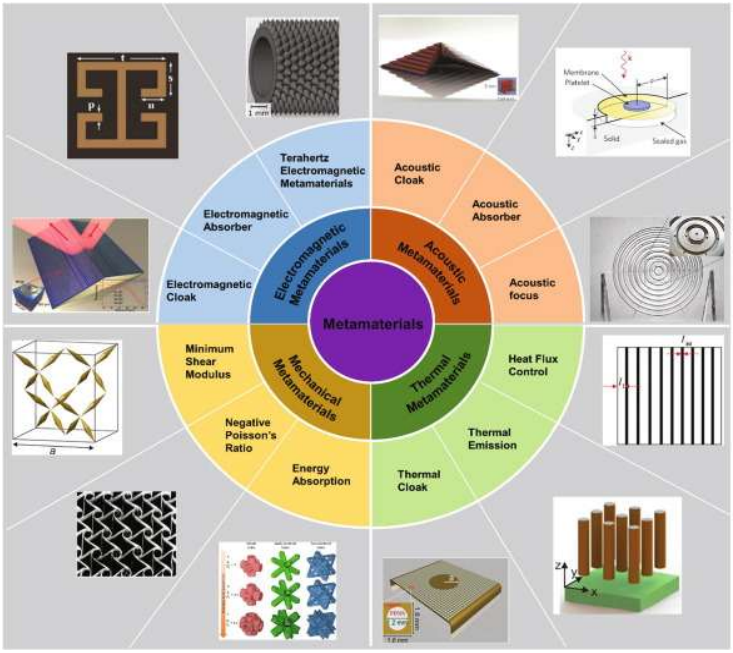


Fig. 8 Various applications of Metamaterial

Research on metamaterials spans many interconnected fields, including electrical engineering, electromagnetics, optics, solid-state physics, microwave and antenna design, optoelectronics, materials science, nanotechnology, and semiconductor engineering. New advances also indicate potential for metamaterials in optical computing, where certain operations might be carried out more efficiently than with traditional computing methods.

1.6 Identified Research Gaps and Challenges

Although metamaterials have demonstrated outstanding capabilities in controlling electromagnetic waves for applications such as sensing, imaging, communication, and absorption systems, several limitations and unresolved issues still exist. These challenges impact their practical implementation, large-scale manufacturing and long-term performance. Thus, researchers are still searching for new design approaches, materials, and optimization techniques to improve the efficiency and applicability of metamaterial-based devices. Below we discuss some of the major research gaps and challenges associated with metamaterials.

1.6.1 Research Gaps

• **Fabrication and Scalability**: The complex fabrication techniques makes the large-scale production of metamaterial sensors more difficult and expensive.

• **Broadband Operation:** Most metamaterial sensors operates efficiently only within a narrow frequency range and have limiting wideband applications.

• **Integration with Other Technologies:** Hybrid sensing systems which combines metamaterials with conventional sensor technologies are still limited.

• **Material Losses:** High metallic and dielectric losses occurs in plasmonic metamaterials which results in reducing sensing efficiency and resonance quality.

• **Flexibility and Miniaturization:** It is reducing sensor size while maintaining high performance and structural stability still a challenge.

• **Lack of Standardization:** The absence of common performance evaluation methods makes comparison between different sensor designs difficult.

• **Sensitivity in Complex Environments:** The sensor performance often degrades in heterogeneous environments such as biological samples etc.

• **Quantitative Sensing Limitations:** Achieving accurate quantitative measurements by including analyte concentration detection remains difficult.

1.6.2 Challenges

• **High Fabrication Cost:** By using advanced microfabrication and nanofabrication methods results in increase of the overall production cost of sensors.

• **Limited Material Availability:** Using suitable low-loss materials for high-performance metamaterial sensor design are still limited.

• **Complex Electromagnetic Simulations:** For accurate modelling in electromagnetic interactions occurs in metamaterial structures requires high computational resources.

• **Environmental Sensitivity:** Various external factors such as humidity, temperature, and electromagnetic interference can affect sensor performance thus become a challenge.

• **Integration with Electronics:** If combining metamaterial sensors with existing electronic and signal-processing systems then this become very difficult.

• **Low Stability under Practical Conditions:** Long-term operational stability and reliability under real-world conditions are still insufficiently explored.

• **Trade-Off between sensitivity and quality Factor:** Improving sensitivity often negatively affects bandwidth or resonance quality.

• **Commercialization Difficulties:** Large-scale industrial implementation of metamaterial sensors remains limited due to manufacturing and cost-related challenges.

CHAPTER 2

RESEARCH OBJECTIVES

1. The current work aims to design a highly sensitive Terahertz (THz) metamaterial based biosensor for the detection of Mycobacterium Tuberculosis (TB). The work focuses on shift in resonance due to even small changes in refractive index when TB analytes interact with the metamaterial.
2. To optimize all structural parameters of the metamaterial unit cell to achieve maximum absorption and minimum Reflection Coefficient.
3. To achieve high sensitivity by providing strong electromagnetic field confinement and measurable resonance shifts for different TB analyte refractive indices.
4. To evaluate key performance metrics such as:
   - FWHM
   - Q-Factor
   - FOM
5. To compare the sensor's performance with previously reported data.

CHAPTER 3

LITERATURE REVIEW

Over the few years metamaterial based absorbers and THz biosensors have become really promising for a lot of different uses like sensing, medical diagnosis, imaging technologies and advanced communication systems. Metamaterial-based absorbers and THz biosensors are getting better and better. To make these devices work better researchers have tried out different shapes for the resonators different materials for the substrates and different structural designs to improve things like how well they absorb how sensitive they are, how wide a range of frequencies they can handle and other important factors. They have also tried to make sure the impedance matches well and that the electromagnetic field is strong and focused and that the device can work at frequencies. The next part will talk about some studies that have been done on metamaterial absorbers and THz biosensing applications.

In the area of TB diagnosis, Ragavan and their team proposed a model for identifying Mycobacterium tuberculosis. This developed system results in excellent classification capability which achieves an accuracy of 99.12 %, along with a sensitivity of 98.74 % and a specificity of 98 % [34]. These results show that this new approach is very promising, for detecting tuberculosis reliably.

In another study, Singh et al. designed a biosensor for the detection of TB cells. The proposed sensor applied a split-square resonator structure with a gap at the end. This was constructed using a dielectric substrate layer made up of polyimide and placed between an aluminium ground layer and a metallic resonator at the top. The designed structure demonstrated notable sensing performance, providing sensitivities of 666 GHz/RIU, 500 GHz/RIU, 333 GHz/RIU, and 250 GHz/RIU for TB1, TB2, TB3, and TB4 samples, respectively [35]. These results show that metamaterial biosensors are really good at finding tuberculosis using terahertz waves.

Recently people have been very interested in metamaterials because they are great at sensing things. This makes them useful for detecting cancer and for biomedical sensing. Saadeldin and his team made a sensitive biosensor in 2019. They used a structure and added a Teflon layer between two gold layers to make it work better. This sensor achieved an absorptivity of 0.99 at a resonance frequency of 2.24 THz. Metamaterial biosensors like this one are very effective for detecting tuberculosis and other diseases. Metamaterials are being used more and more for these kinds of applications because they are so good, at sensing things. Also, the device shows a maximum sensitivity of 300 GHz/RIU, a figure of merit (FOM) of 2.94 RIU^{-1}, and a quality factor (Q-factor) of 22.05 which indicate the strong sensing performance [36].

Later, Patel and his team (2022) introduced a graphene-based metamaterial biosensor which was designed to detect various cancerous cells. The structure consisted of a split-ring resonator on a glass substrate, where graphene was incorporated to improve the sensing response. The sensor achieves a sensitivity of 207.14 GHz/RIU along with a Q-factor and FOM of 13.11 and 3.86 RIU^{-1} respectively which highlights its potential for various sensing applications [37].

Guo and his team proposed a kind of biosensor in 2023. This biosensor uses a geometry called an open square ring resonator and it is made with copper. They used lead glass as the dielectric spacer layer. The proposed structure promising sensing characteristics which achieves a Q-factor of 79.26, a sensitivity of 91.50 GHz/RIU, and figure of merit (FOM) of 11.97 RIU^{-1} [38].

Qu and his team made a kind of sensor in 2023. This sensor is made with a material and has four identical square rings on a lead base. The sensor works well with a high Q-factor of 55.3. It is also very sensitive with 78.6 GHz/RIU. Has a good figure of merit of 9.81 RIU^{-1} [39].

In 2023 Zhang and his team made another kind of sensor. This sensor can detect two frequencies and works with any kind of light polarization. It has a ring shape, with two openings and is made of gold. The ring is placed on a spacer made of Polytetrafluoroethylene, which is a kind of plastic. The proposed sensor achieves an average refractive index (RI) sensitivities of 163 and 488 GHz/RIU for the two resonance bands. Figure of merit (FOM) values were reported as 5.09 and 9.04 RIU^{-1}, while the obtained Q-factors were reported as 22.8 and 40.7, respectively [40].

Later, Aliouar et al. [2025] developed a terahertz metamaterial biosensor employing gold as the metallic layer and polyimide as the substrate material. The proposed structure consisted of a rectangular resonating element placed at the center and surrounded by a ring-shaped geometry. The sensor exhibited excellent absorption performance of 99.97 % at a resonance frequency of 2.96 THz. Furthermore, the device achieved a maximum average sensitivity of 600 GHz/RIU, along with a FOM of 60 RIU^{-1} and a high Q-factor of 296.90 [41].

In another investigation, Tammam et al. [2025] developed a flexible THz metamaterial sensor aimed at hemoglobin (Hb) monitoring and the early identification of cancer. The proposed sensor achieved a high absorptivity of 98 % at a resonance frequency of 1.1 THz, along with an average sensitivity of 556.3 GHz/RIU and a quality factor of 13.2 for cancer detection applications [42].

Zhang et al. [43] introduced a terahertz (THz) metamaterial biosensor which was used to coupled resonator structures for the classification of glioma cell. The proposed sensor report a theoretical sensitivity of 496.0 GHz/RIU and was experimentally capable of differentiating between mutant and wild-type glioma cells.

Further improvements in sensing accuracy, stability, and reliability are still needed before terahertz biosensors can be widely used in real biomedical diagnostic applications.

CHAPTER 4

SIMULATION SOFTWARE

In our work we analyzed the proposed structure using a special software called CST Studio Suite. This software uses a method called finite element method (FEM) to solve problems in the frequency domain. This method is good for studying how electromagnetic waves interact with materials in the THz region. The Frequency-Domain Solver in the software helped us study how the designed structure behaves at frequencies absorbs energy and distributes electric fields. This approach helps us examine and optimize performance parameters.

This numerical approach gives information of key performance parameters like resonance frequency, sensitivity, quality factor, and detection accuracy. Therefore, the simulation setup helps improve the performance and stability of the THz metamaterial biosensor for biomedical sensing applications.

4.1 CST STUDIO SUITE

CST Studio Suite is a widely used software for the design and analysis of high frequency and microwave devices. It helps researchers understand the behavior of electromagnetic waves and simulate structures working in the microwave, millimeter wave, and terahertz (THz) regions. The software applies numerical techniques to obtain accurate results for complex electromagnetic studies.

The software provides a 3D simulation platform where different structures such as antennas, resonators, waveguides, metamaterials, and biosensors can be designed and analyzed. It allows the study of several electromagnetic properties, including resonance frequency, absorption, transmission and reflection coefficients, and electric field

distribution. In this work, the simulated S parameters were used to determine absorptivity. The shift in resonance frequency at different refractive index values was further used to evaluate the sensitivity of the proposed biosensor.

For metamaterial biosensor applications, CST Microwave Studio is useful for studying the interaction between electromagnetic waves and different material structures. It also supports material models like the Drude model, which is commonly used for tunable materials such as Vanadium dioxide. Due to its accuracy, flexibility, and visualization capability, CST Microwave Studio is widely applied in terahertz and electromagnetic research.



Fig. 9 Computer Simulation Technology Logo

4.2 Numerical Approach used in CST Studio Suite

The simulation software used advanced algorithms for the numerical analysis of the proposed biosensor designs and to check their overall performance. These tools use mathematical techniques to perform a detailed evaluation of their characteristics and behavior. The main method used for this analysis is explained in the section.

Finite Element Method (FEM)

The Full Vector Finite Element Method (FEM) is a numerical technique which is used in CST Studio Suite for designing and analysing the metamaterial biosensors. In this method, the whole simulation area is divided into many small parts therefore are known as finite elements or meshes. Maxwell's electromagnetic equations are solved in these small sections to study structures with complex geometry and different material properties accurately. The method calculates all components of the electric and magnetic fields, including Ex, Ey, Ez, Hx, Hy, and Hz. After solving each element, the complete electromagnetic response of the sensor is obtained by combining all the results.

For THz metamaterial biosensors, FEM is useful for studying how electromagnetic waves interact with the resonator structure. It helps in analyzing important parameters such as resonance frequency, electric and magnetic field distribution, absorption, transmission, reflection, and sensing performance.

Also they uses adaptive meshing to improve the accuracy. The mesh becomes finer in regions only where strong field variation occurs. This improves the precision of the simulation while reducing unnecessary computational effort. The thing about FEM is that it really works well for making biosensor designs better. FEM is great for getting sensitivity from biosensors. It also helps to improve the quality of biosensors.. It makes the sensing characteristics of biosensors better. So FEM is very useful for optimizing biosensor designs to get the results, from biosensors. FEM helps to make biosensors more effective.

CHAPTER 5

NUMERICAL ANALYSIS

5.1 Introduction

This chapter presents the numerical and computational analysis of the proposed THz metamaterial biosensor which is designed for the detection of tuberculosis using CST Studio Suite. The performance of the sensor and its electromagnetic behavior are studied using the finite element method (FEM). This method helps in accurately examining the resonance response, field distribution, and interaction between the sensor structure and the target sample. During the simulation study to observe the sensing response of the biosensor different refractive index values are used. The proposed design is further judged through important performance parameters such as absorption, sensitivity, Q factor, and figure of merit (FOM). These parameters help in understanding the sensing accuracy, selectivity, and also the overall efficiency of the biosensor for future THz biomedical sensing applications.

5.2 Mathematical modelling

1. Absorption capability:

The absorption performance is a factor in how well it absorbs electromagnetic radiation at a specific frequency. This connection helps improve sensing efficiency. The absorption performance directly impacts its ability to efficiently absorb radiation. When absorption is high the interaction between the waves and the material is stronger leading to sensing results. The materials design plays a role in achieving high absorption performance. It helps in absorbing electromagnetic radiation at the resonant frequency. The absorptivity of the structure is determined from the transmission and reflection coefficients, where near-perfect absorption is achieved when both transmission and reflection are minimized

at the resonance frequency. The absorption capability (A) of the proposed metamaterial structure was determined using the following expression:

$$A(\omega) = 1 - R(\omega) - T(\omega) \quad (3)$$

In this equation, R(ω) and T(ω) represent the reflection and transmission coefficients, respectively. By analyzing these coefficients, the absorption behaviour of the designed metamaterial biosensor can be effectively examined. The reflection coefficient is calculated as $R(\omega)=|S_{11}|^2$ whereas the transmission coefficient is given by $T(\omega)=|S_{21}|^2$.

Here, S_{11} corresponds to the reflection amplitude coefficient, while S_{21} denotes the transmission amplitude coefficient of the proposed structure.

As the ground plane of the proposed unit cell is composed of gold, a highly conductive material, the transmission of EM waves through the metamaterial (MM) structure becomes nearly negligible, while the reflected waves are also considerably minimized. Consequently, the majority of the incident THz radiation is effectively absorbed by the structure, preventing the THz waves from propagating through the absorber. Therefore, the transmission coefficient can be approximated as $S_{21}=0$. Under this condition, the absorption capability (A) of the proposed structure can be expressed as:

$$A = 1 - |S_{11}|^2 \quad (4)$$

2. Drude Model for VO_2:

The electromagnetic response of VO_2 is modeled using the Drude model, which describes the interaction of free charge carriers with incident THz waves. This model helps in studying how the dielectric properties and conductivity of the material change with frequency under different conditions. The numerical results give a clear understanding of the sensor behavior. They also show that the proposed THz metamaterial biosensor can be effectively used for sensitive tuberculosis detection.

The complex permittivity of VO_2 can be expressed as:

$$\varepsilon(\omega) = \in_{\infty} - \frac{\omega_p^2}{(\omega^2 + i\gamma\omega)} \quad (5)$$

In this expression, $\in_{\infty}$ denotes the dielectric constant at high frequency and is set to 12, ω_p corresponds to the plasma frequency, γ represents the collision frequency assumed to be 5.75×10^{13} rad/s, and ω *is* the angular frequency of the incoming THz radiation [44].

The plasma frequency (ω_p) is directly influenced by the electrical conductivity (σ) of the material. As the conductivity changes, the plasma frequency also varies accordingly. Their relationship can be expressed as:

$$\omega_p^2(\sigma) = \frac{\sigma}{\sigma_o}\, \omega_p^2(\sigma_o) \quad (6)$$

Where, σ_o represents the reference conductivity, while $\omega_p(\sigma_o)$ denotes the plasma frequency corresponding to that reference conductivity. This equation indicates that the square of the plasma frequency is proportional to the conductivity of the material.

3. Sensitivity:

Sensitivity describes the capability of the sensor to detect the minor changes in the refractive index of the analyte. In our study, sensitivity is analyzed by checking the variation in resonance frequency when the refractive index of the sensing medium changes. A larger shift in the resonance frequency results into enhanced sensing efficiency and improved detection accuracy.

The sensitivity is determined as the ratio of change in the resonance frequency shift and the corresponding change in refractive index, which is commonly measured in unit GHz/RIU.

$$S = \frac{\Delta f}{\Delta n} \quad (7)$$

Where, S represents the sensitivity, Δf denotes the shift in the resonance frequency, and Δn denotes the variation in the refractive index.

4. Quality-factor:

The quality factor (Q-factor) parameter describes the sharpness and strength of the resonance response. A larger Q-factor means it corresponds to a narrow resonance bandwidth and it improved the confinement of electromagnetic energy within the resonator. This results in higher sensing precision and better capability to detect the small variations.

The Q-factor is determined as the ratio of the resonance frequency to the full width at half maximum (FWHM) of the resonance peak.

$$Q - factor = \frac{f_o}{FWHM} \tag{8}$$

where, f_o represents the resonance frequency corresponding to a particular value of the refractive index.

5. Figure of Merit (FOM):

Figure of Merit (FOM) is used to measure the sensing performance and detection capability. A larger FOM value signifies that the sensor can identify very small changes in refractive index which then improved the accuracy and stability of the biosensor.

FOM is also defined as the ratio of sensitivity and the value of FWHM.

$$FOM = \frac{S}{FWHM} \tag{9}$$

CHAPTER 6

DESIGN AND METHODOLOGY

The conventional metamaterial (MM) absorbers generally consist of three different layers: a metallic ground layer at the bottom, a dielectric substrate layer placed in the middle, and a patterned resonator layer on the top. Different resonator structures are added to the top layer to improve impedance matching with free space. This greatly reduces reflection loss [45]. Numerical simulations were performed using CST Simulation Studio to optimize the proposed structure and investigate its optical characteristics. The adopted approach making it a good absorber and a biosensor by maintaining high sensitivity toward variations in the refractive index through detailed parametric analysis.

6.1 Description of unit cell and Periodic boundary conditions

The proposed THz absorber is designed in the form of a 3 × 3 unit-cell array, as illustrated in the figure 10 (a). Each unit cell possesses a periodicity of 100 μm along both the x- and y-directions (Px = Py) and consists of a tri-layer metal-insulator-metal (MIM) structure with a bottom gold reflector, a middle paper dielectric spacer, and a top VO_2 resonator consists of three closed circular ring resonators placed between two rectangular bricks. Figure 10 (b), and (c) present the three-dimensional schematic diagram, front view of the proposed metamaterial unit cell respectively.

The structural design and numerical simulations were performed using CST Microwave Studio. In the simulation setup, unit cell boundary conditions were applied along the x- and y-directions, while open boundary conditions with additional space, equivalent to a perfectly matched layer (PML), were assigned along the z-direction to minimize unwanted reflections. A planar electromagnetic (EM) wave was normally incident from the top surface along the z-axis, ensuring that the electric and magnetic field components remained mutually perpendicular [46]. Furthermore, tetrahedral meshing was employed to improve the accuracy of the simulation, and the frequency-domain solver was utilized

to investigate the electromagnetic response of the proposed structure. During the analysis, the magnetic field and electric field polarizations were maintained along the x-axis and y-axis, respectively.

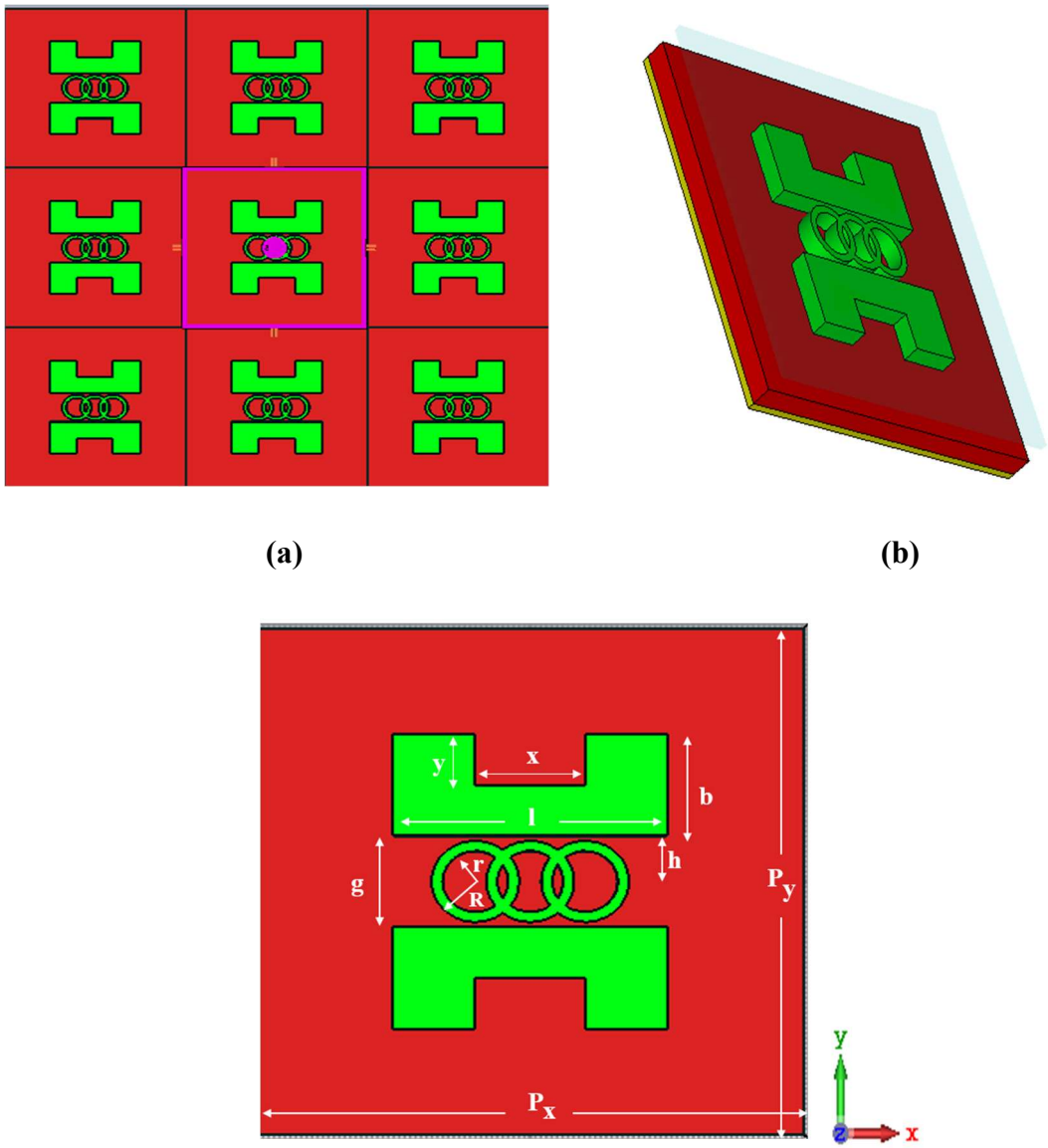
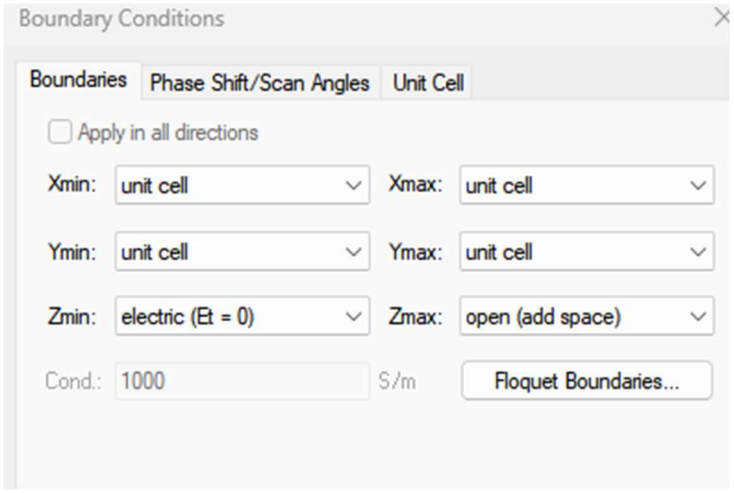
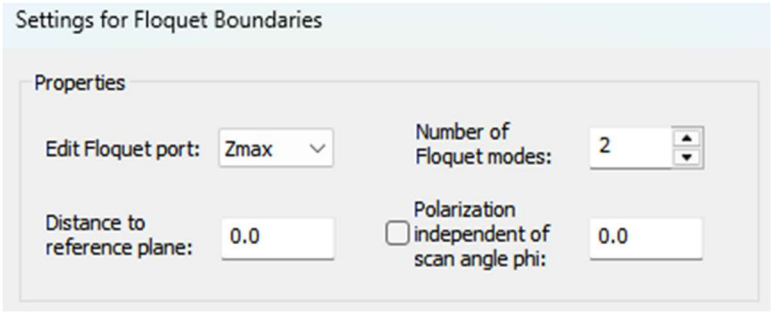


Fig.10 (a) Layout of 3×3 unit cell array of the proposed THz biosensor **(b)** Three-dimension schematic diagrams of the unit cell **(c)** The structural configuration and the front view of unit cell



(a)



(b)

Fig.11 Simulation model demonstrating the use of **(a)** periodic boundaries and **(b)** Floquet port settings applied in proposed unit cell

6.2 Choice of materials

In the development of a metamaterial biosensor, the choice of materials for different layers plays a crucial role, as the overall sensing performance strongly depends on the electromagnetic characteristics, absorption efficiency, and tunable behavior of the structure. In the proposed design, gold is used in the bottom metallic layer, paper material is used as the dielectric substrate layer in the middle, and vanadium dioxide (VO_2) used in the top resonator layer.

- Gold is selected for the bottom layer due to its high electrical conductivity of 4.56×10^7 S/m and also due to its excellent chemical stability [45]. Gold works well in the THz frequency range as it helps to reflect waves so they do not go through the structure and that makes the absorption performance better. It is also good because it has ohmic losses and it supports strong plasmonic effects, which means the sensor can detect things more clearly and it has better sensing characteristics. Also one more fact that make gold a suitable option is that it does not oxidize or corrode easily which makes the biosensor more stable and reliable over time. That is very important, for the gold biosensor.

- Paper is used as the dielectric substrate because it offers several properties like low dielectric loss, flexibility, lightweight structure, and low fabrication cost etc. It has a dielectric constant of 2.31, loss tangent of 0.003, density (ρ) of 800 kg/m³, thermal conductivity of 0.05 W/K/m, and thermal diffusivity of 4.46×10^{-8} m²/s [45]. Also paper material is safe for the environment. It is also biocompatible. This makes paper a good choice, for sensing applications.

- Vanadium dioxide is selected for the top layer because it has good electromagnetic properties and it is good at dealing with THz radiation. It also has high electrical conductivity. This means it can make resonance and keep the electromagnetic fields inside the metamaterial structure really well. So the biosensor we are proposing can absorb things better. Sense things more efficiently. Vanadium dioxide also has the advantage of low

optical losses. This makes it a good material for making powerful THz devices. The material helps make resonance responses that're sharp and stable. This is helpful because it means we can get a quality factor be more sensitive and detect things more precisely. Because of all these things Vanadium dioxide is a great material to use for making advanced biosensors that are used to sense things in the body.

6.3 Methodology of Design

The proposed unit cell was designed using various optimized geometric shapes to enhance the interaction with electromagnetic waves and to improve the absorption performance.

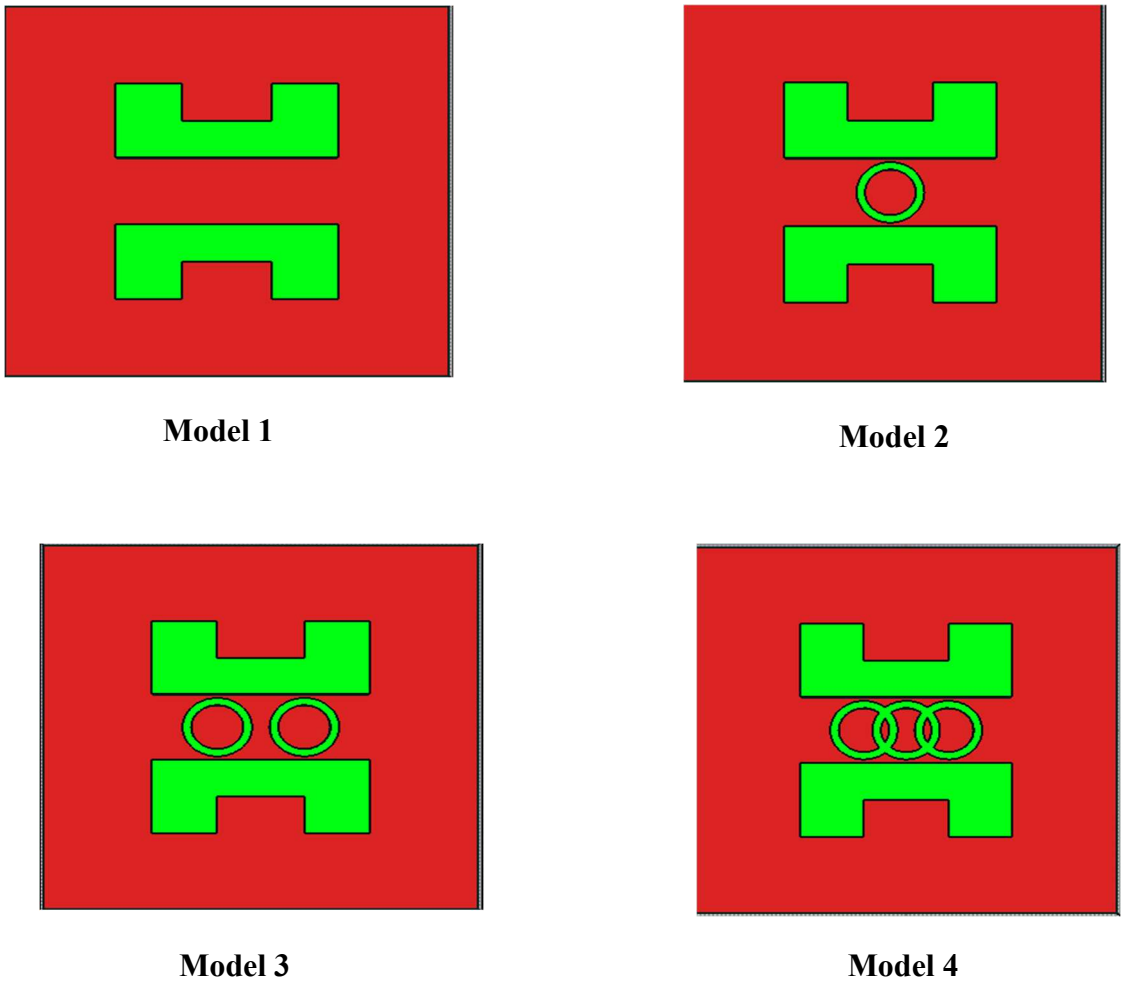


Fig.12 Design generation of proposed unit cell

To study how the resonator arrangement affects the absorber characteristics, we examined four different structures by changing the number of circular closed ring resonators placed between the rectangular brick shaped elements, as illustrated in Fig. 12. Each structure was analyzed in detail in this section.

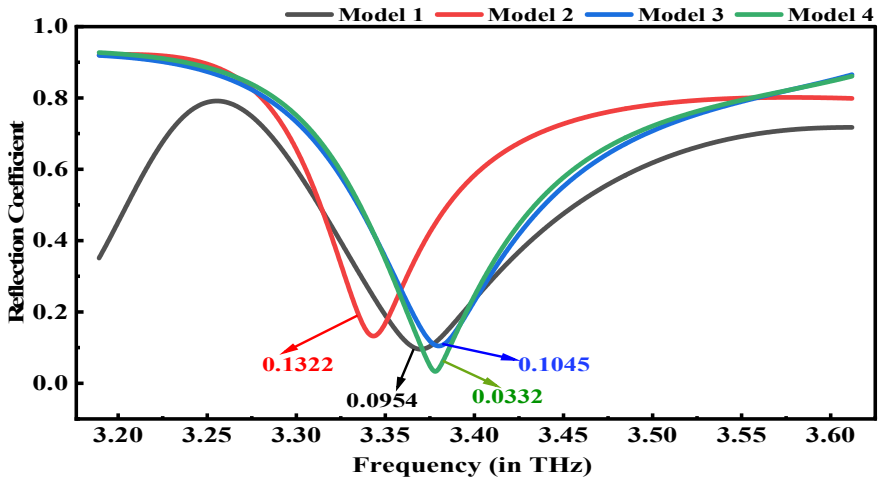
In Model 1, we used only rectangular bricks without any circular ring resonators. This structure results into low reflection coefficient of 0.0954 and a high absorptivity of 99.08 %. Even though the absorptivity value is high but the absence of ring resonators limited the overall electromagnetic field confinement and resonance enhancement occurs within the structure.

In Model 2, we introduced a single circular ring resonator between the rectangular bricks to improve the interaction. However, the use of only one ring increased the reflection coefficient to 0.1322 but slightly decreasing the absorptivity to 98.25 % as compared to Model 1. This results shows that a single resonating element was not sufficient in order to provide effective impedance matching or strong resonance coupling.

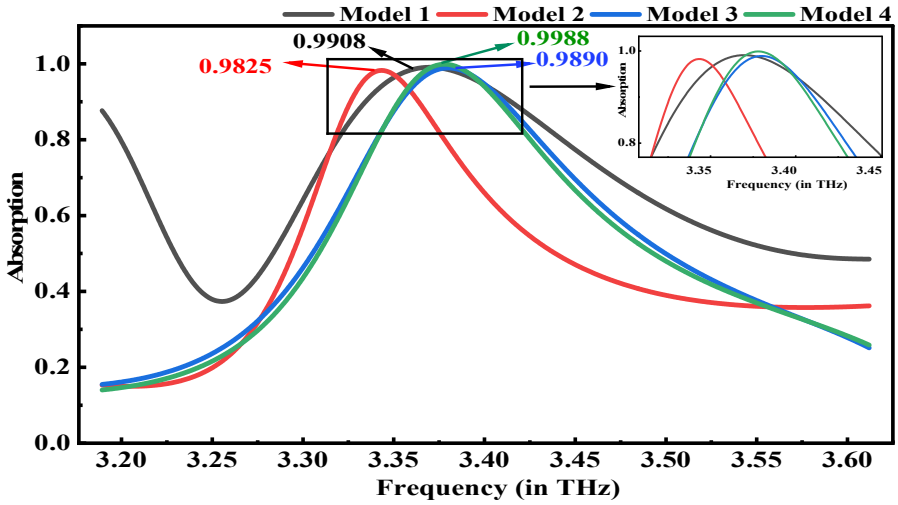
To enhance the performance further, we used two circular ring resonators in between the rectangular bricks as shown in Model 3. Here, the reflection coefficient reduced to 0.1045 and the absorptivity improved to 98.9 %. Although the extra ring improved the confinement of field and also enhanced the electromagnetic interaction but the increase in absorption was still limited. This shows that the resonance characteristics and surface current distribution were not yet completely optimized.

Finally, a significant improvement in absorber performance was achieved in the proposed Model 4, where three intersecting circular ring resonators were incorporated between the rectangular bricks. The presence of multiple intersecting rings greatly enhanced the resonance effect and improved the impedance matching characteristics of the structure. Consequently, the absorptivity increased sharply to 99.88 %, while the reflection coefficient dropped to 0.0332. The enhanced performance can mainly be attributed to

stronger localization of electromagnetic fields, improved surface current distribution, and the generation of multiple resonance modes due to the intersecting ring arrangement. In Fig.13 the simulated results for reflection coefficient and absorptivity for all the models are shown.



(a)



(b)

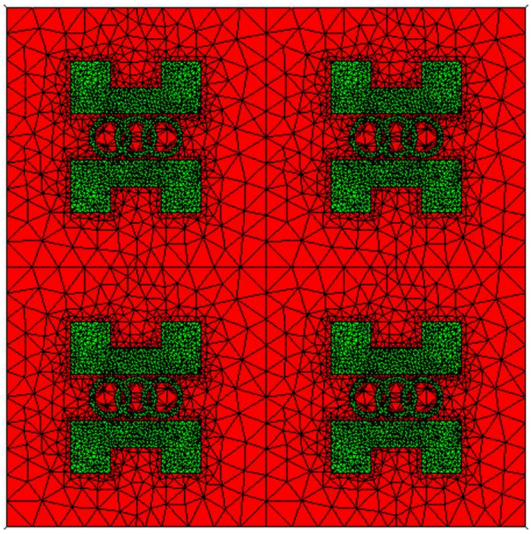
Fig.13 Enhancement of the proposed absorber and response characteristics at various stages of absorber development **(a)** Reflection response and **(b)** Absorption characteristics.

6.4 CST simulation setup parameters (mesh type, ports, monitors)

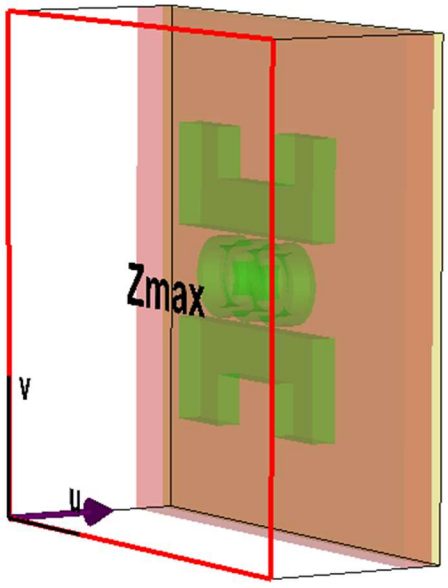
- **Mesh Type:** A tetrahedral mesh with adaptive refinement was employed to accurately capture the intricate geometrical details and variations in the electromagnetic field distribution.

- **Ports:** To excite the metasurface, two floquet port were applied, allowing plane-wave illumination during the simulation process.

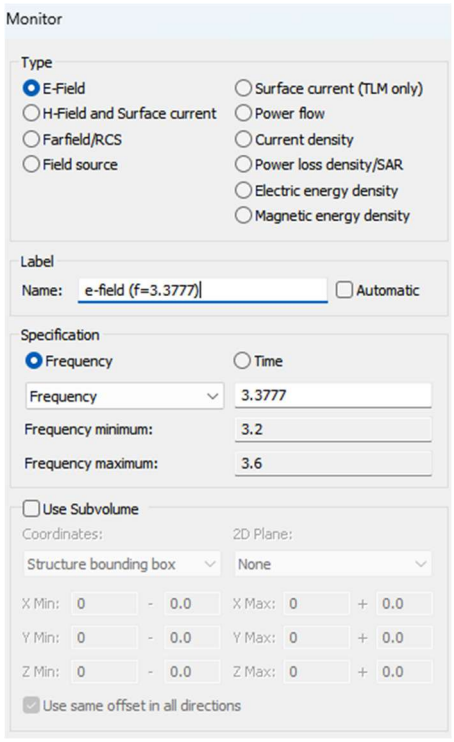
- **Monitors:** Frequency-domain monitors were utilized to observe and analyze important parameters such as absorption characteristics, reflection response, and near-field distributions at selected operating frequencies (3.2 -3.6 THz).



(a)



(b)



(c)

Fig.14 (a) Showing mesh view of the proposed metamaterial biosensor **(b)** Port setup used for electromagnetic wave excitation **(c)** Frequency monitor setup for various analysis

The proposed structure was analyzed using the Finite Element Method (FEM) solver. Periodic boundary conditions were applied along both the x- and y-directions to represent the repeating nature of the design. Along the propagation direction (z-axis), a perfect electric conductor boundary condition (Et=0) was assigned at the Zmin plane for the normally incident plane wave. In contrast, the Zmax plane was treated as an open boundary with extra space provided to ensure accurate wave propagation and proper electromagnetic interaction within the structure.

CHAPTER 7

PARAMETRIC OPTIMIZATION AND ANALYSIS

This section explains the parametric study of the proposed structure (Model 4) to find the optimum design parameters. Optimization was done by varying the different parameters given in Table 1, such as substrate thickness, resonator thickness, and circle radius, individually while the other parameters were kept unchanged. Our aim was to achieve near-perfect absorption. The effect of these parameter changes can be seen in Figures 15-18.

Figure 15 shows how the substrate thickness ($t_{substrate}$) affects the performance of the proposed structure. The thickness was changed from 4 μm to 8 μm with a step of 2 μm. The results show that increasing the substrate thickness causes a red shift in the resonance frequency. This indicates that the interaction between the electromagnetic waves and the structure strongly depends on the dielectric layer thickness. Changes in absorption are also observed. The absorption values are 69.79%, 99.14%, and 94.64%, respectively. The maximum absorption is obtained at 6 μm. This happens because the impedance matching between the absorber and free space becomes better.

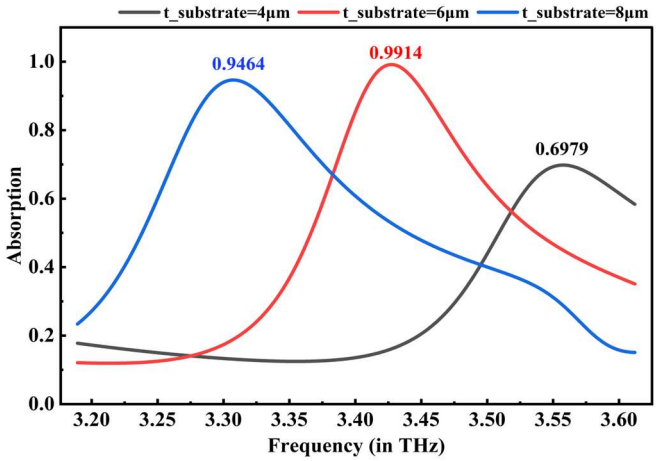


Fig.15. Geometric parameter: Variation in substrate thickness

As a result, reflection loss decreases and the electromagnetic field remains more confined inside the structure. When the substrate thickness is increased further, the absorption starts to decrease due to weaker field confinement.Therefore, the substrate thickness of 6 µm was selected as the optimized value since it provides the maximum absorptivity of 99.14 %.

Figure 16 shows the effect of changing the resonator thickness ($t_{resonator}$) from 2 µm to 6 µm with an interval of 1 µm. The obtained absorption values are 80.83 %, 93.26 %, 99.14 %, 99.81 %, and 97.72 %, respectively. The results indicate that the absorption increases noticeably as the resonator thickness rises up to 5 µm. But when the thickness exceeds 5 µm, the absorption starts decreases. From these results we conclude that among all the tested values, the maximum absorption of 99.81 % is obtained at 5 µm. Therefore, 5 µm was selected as the optimized resonator thickness for the proposed biosensor.

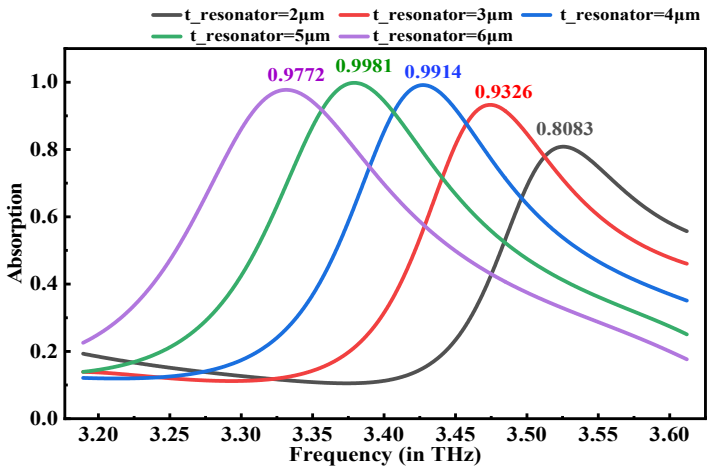


Fig.16. Geometric parameter: Variation in resonator thickness

Similarly, the value of the inner radius of the circular resonator (r) was judged by changing its value from 4 µm to 10 µm in steps of 2 µm, as shown in Figure 17. The obtained absorption values are 99.38 %, 99.81 %, 97.79 %, and 92.26 %, respectively. These results demonstrate that the geometrical dimensions of the circular resonator strongly affect the resonance intensity and electromagnetic field localization. Initially, increasing the radius

improves resonance coupling, leading to enhanced absorption performance. However, further enlargement of the radius weakens the interaction between incident wave and the structure and reduces the absorption efficiency. Therefore, the optimum inner radius was determined to be 6 μm, where the maximum absorption of 99.81 % was achieved.

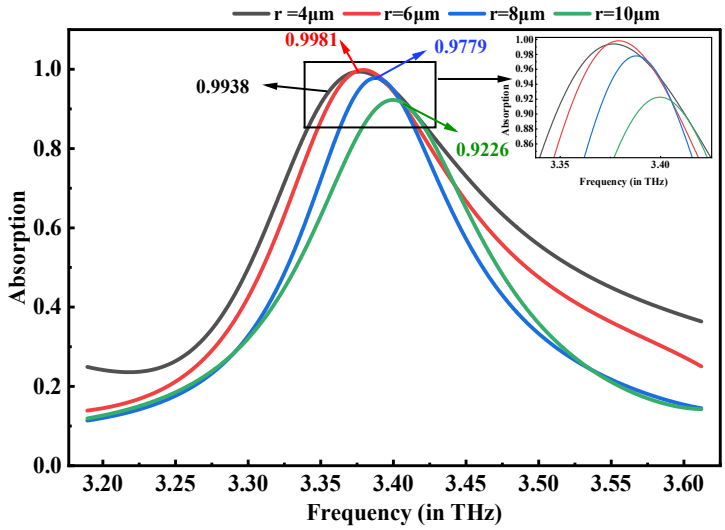


Fig.17. Geometric parameter: Variation in inner radius of circular rings

In addition, figure 18 illustrates the influence of the half distance between the two brick-shaped resonating structures (h), which was varied from 8 μm to 12 μm with a step size of 1 μm. The results show that the spacing between the resonating elements directly affects the electromagnetic coupling and near-field interactions within the structure. Among all the tested configurations, the highest absorption peak of 99.81 % is obtained at 9 μm, indicating the strongest resonance coupling at this separation distance. When the spacing is increased further, the interaction between the resonating elements becomes weaker, slightly reducing the absorption efficiency. Hence, the optimized half-gap distance was selected as 9 μm, corresponding to a total separation of 18 μm between the two rectangular brick-like structures. Finally, Table1 summarizes the optimized geometrical parameters of the proposed absorber design. These optimized dimensions were subsequently utilized

for further simulation studies and performance evaluation of the THz metamaterial biosensor.

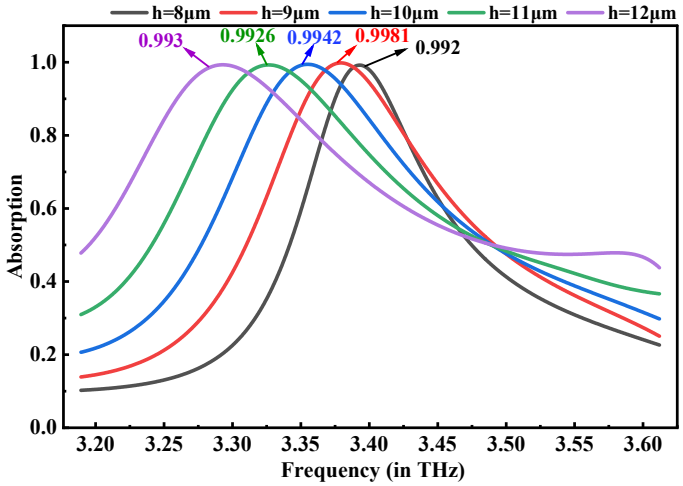


Fig.18. Geometric parameter: Variation in half gap between bricks

Table1. Optimized parameter for the proposed Design

Name	Value(µm)	Description
t_ground	2	Height of ground
t_substrate	6	Height of substrate
l	50	Length of brick
b	20	Breadth of brick
g	18	Distance between bricks
h	9	Half distance between bricks
t_resonator	5	Height of resonator
$P_x = P_y$	100	Length and breadth of unit cell
r	6	Inner radius of circular rings
R	8	Outer radius of circular rings
t_analyte	2	Thickness of analyte
x	20	Length of rectangular brick
y	10	Breadth of rectangular brick

CHAPTER 8

ELECTROMAGNETIC FIELD DISTRIBUTION

To gain a deeper understanding of the absorption behaviour of the proposed metamaterial structure, the distributions of both electric and magnetic fields were examined at three different frequency conditions, namely below resonance, at resonance, and above resonance frequencies. The simulation results are shown in figures 19 and 20, which shows how the incident electromagnetic waves interact with the resonator geometry at different operating frequencies.

The figures 19(a), 19(b) and 19(c) show us the field distributions of magnetic field at different frequencies. We see the field distributions at 3.3414 THz, then at 3.3777 THz which is the resonance frequency and finally at 3.4658 THz. At the resonance frequency the magnetic field is very strong around the edges of the ring resonators. It is also strong near the sections of the brick-shaped elements. This happens because the metallic layer and the ground plane are connected in a way that they make parallel surface currents between the two metallic layers. This results in a strong magnetic field inside the dielectric region. The magnetic field is trapped inside the structure. This is important for the structure to absorb energy effectively. The magnetic field distributions at the resonance frequency are very important for the structure to work properly. The figures 19(a), 19(b) and 19(c) help us understand the field distributions, at different frequencies especially at the resonance frequency of 3.3777 THz.

But on the other hand, we observed the magnetic field intensity becomes much weaker at frequencies below and above resonance, as shown in figures 19(a) and 19(c). At these frequencies, the electric field becomes weaker because the surface current excitation is low. This reduces the interaction between the incoming wave and the resonator. As a result, a smaller amount of electromagnetic energy remains trapped inside the structure.

Thus, we noticed the decrease in absorption performance when the system moves away from the resonance frequency.

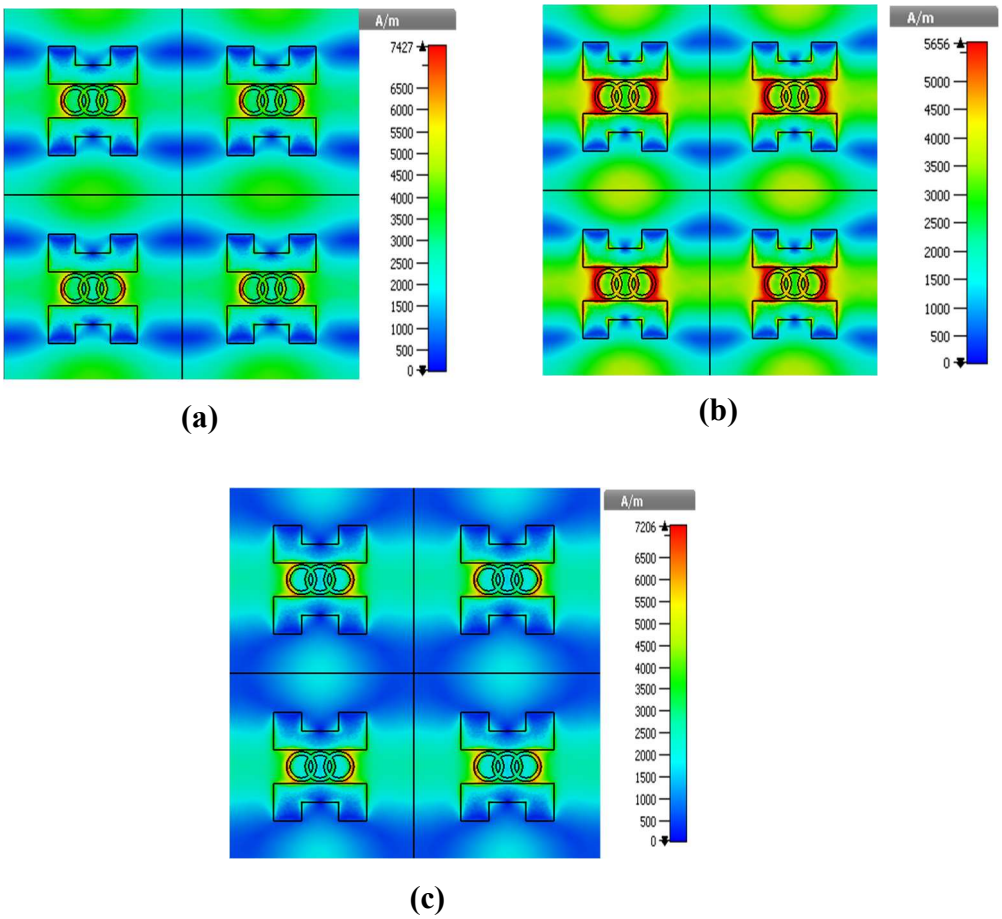


Fig.19 Real |H| -field distribution at: **(a)** 3.3414 THz **(b)** 3.3777 THz (Resonance Frequency) **(c)** 3.4658 THz

Similarly, Figures 20(a), 20(b), and 20(c) show the electric field distributions corresponding to the same frequencies we talked earlier. At 3.3414 THz (below resonance frequency), only a small amount of electric field concentration is observed which is along the outer boundaries of the brick structures. This is clearly shown in Figure 20(a). At the resonance frequency of 3.3777 THz, a very strong electric field is observed near the edges of the brick structures and inside the gap between the closed ring resonator and the bricks, as shown in Figure 20(b). The concentration of the electric field in these regions indicates

strong resonance and better interaction between the incoming electromagnetic wave and the resonator structure. Due to this effect, maximum absorption is achieved. In comparison, at 3.4658 THz, the electric field strength reduces clearly and is mainly limited to the upper part of the central ring resonator, as presented in Figure 20(c). This shows that the resonance becomes weaker at frequencies above the operating range.

Thus we can say that the combined behaviour of the electric and magnetic field distributions confirms that both resonances work together to improve the absorption efficiency of the proposed design.

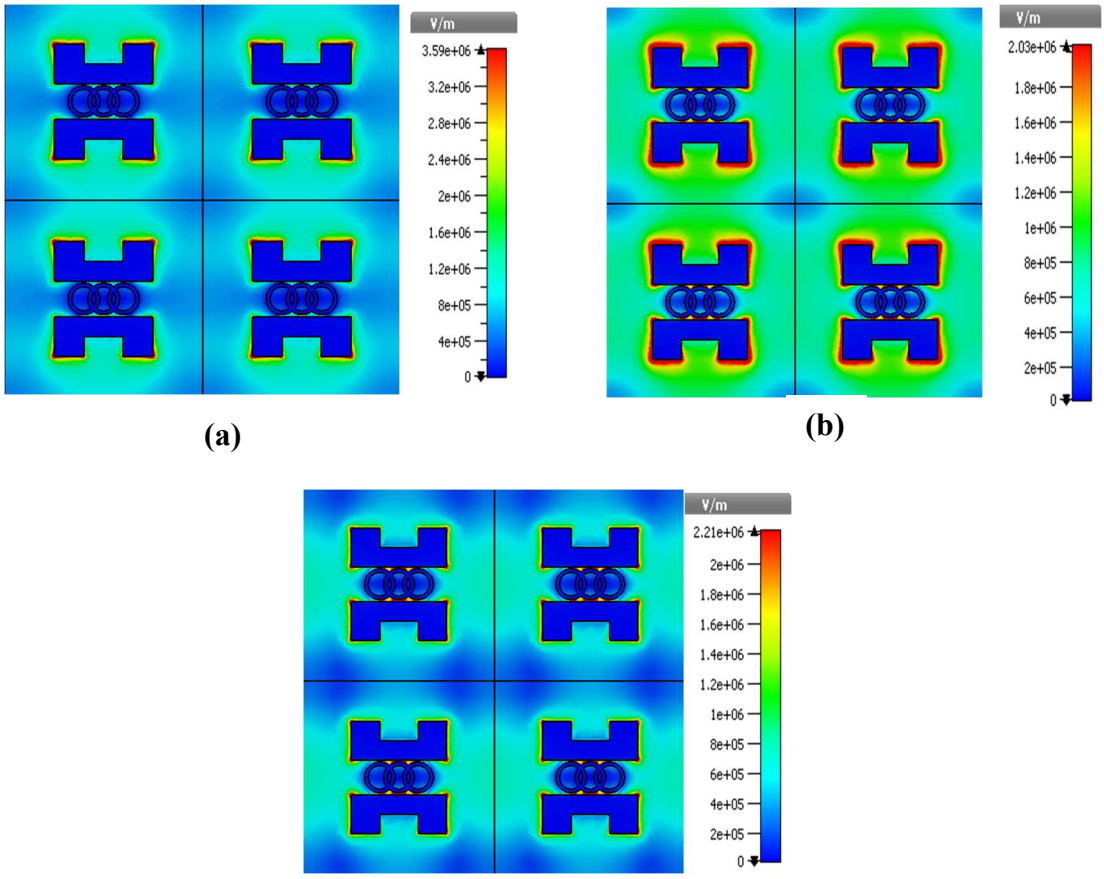


Fig.20 Real |E|-field distribution at: **(a)** 3.3414 THz **(b)** 3.3777 THz (Resonance Frequency) **(c)** 3.4658 THz

From the above discussion we conclude that at the resonance frequency i.e. 3.3777 THz, both the electric and magnetic fields become highly concentrated within the resonator structure. This field confinement shows a strong interaction between the incident electromagnetic wave and the metamaterial surface which leads to high efficient energy absorption. The observed behaviour confirms the ability of the proposed design to achieve near-perfect absorption at 3.3777 THz, which is also shown in figure 21.

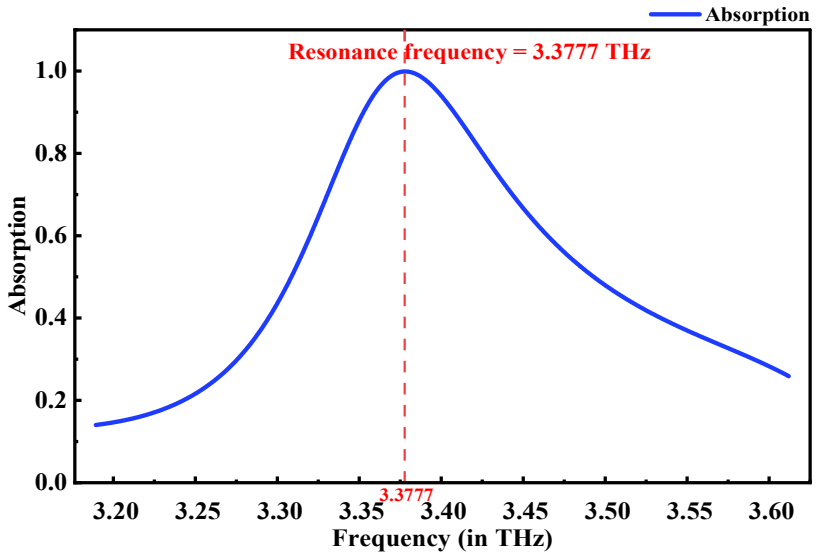


Fig.21 Absorption characteristics of the proposed metamaterial unit cell

CHAPTER 9

RESULTS AND DISCUSSION

9.1 EVALUATION OF REFRACTIVE INDEX SENSOR

A 2 μm thick analyte layer is placed above the resonator so that the proposed absorber can now be used as a sensor. By changing the refractive index (RI) of the surrounding medium this behaviour is studied and observing the changes in the absorption spectrum, as shown in fig. 22(a). The RI is changed from 1.31 to 1.40 with an interval of 0.01 to examine the sensor performance under different conditions. It is found that when the refractive index increases, the absorption resonance shifts towards lower frequencies or higher wavelengths. This shows a clear redshift behaviour. This continuous shift confirms that the proposed structure can detect even small variations in the surrounding refractive index.

The resonant frequencies for different refractive index values are given in Table 2. The results indicate that the resonant frequency continuously decreases when the refractive index increases. This shows a strong interaction between the electromagnetic field and the analyte layer. To study the sensing performance of the proposed structure, a linear fitting was carried out between the refractive index values and the resonant frequencies obtained from the simulation results. Figure 22(b) shows an excellent linear relationship with a coefficient of determination of ($R^2 = 0.993$). The fitted equation is expressed as:

$$f = -0.24703 \times RI + 3.61653 \quad (10)$$

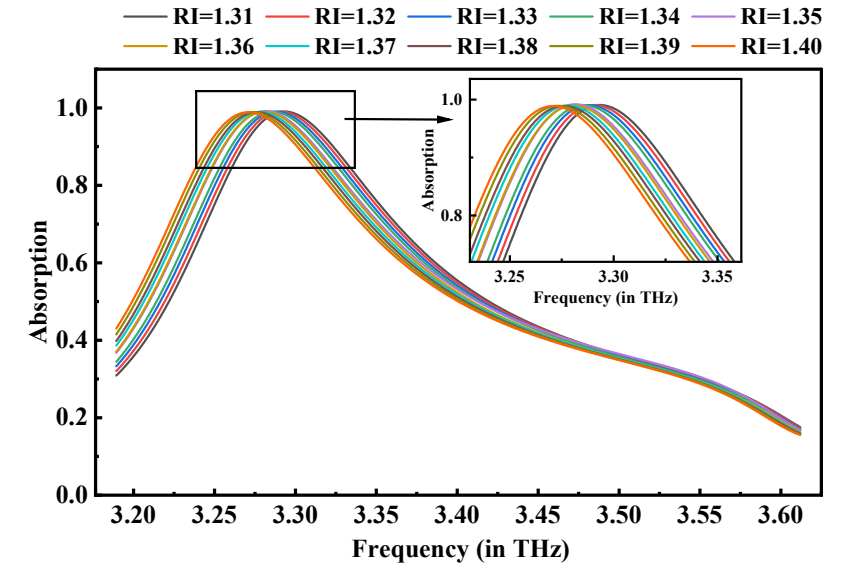
The negative slope of the fitted equation indicates that the resonant frequency decreases from 3.2933 THz to 3.2709 THz as the refractive index changes from 1.31 to 1.40. This inverse relationship proofs the stable and predictable sensing behaviour of the proposed structure. The strong linearity between RI and resonant frequency highlights the suitability of the absorber for refractive index sensing applications. Also, the enhanced confinement

of electromagnetic waves around the resonator improves the interaction between the analyte and the sensing structure. This contributes to the improved sensitivity of the device.

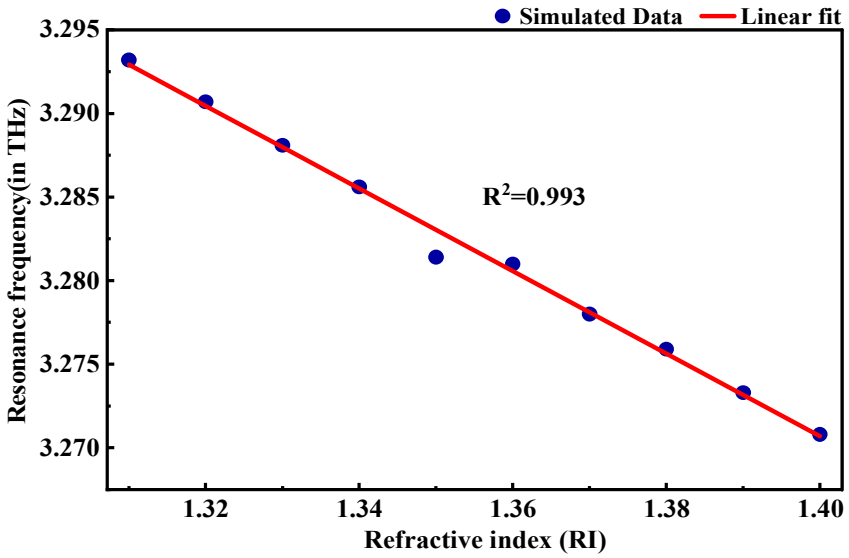
Due to its high sensitivity, the proposed sensor is capable of detecting very small refractive index variations produced by biomolecular interactions. This capability makes the structure highly effective for identifying the changes occurs in biological samples with greater precision. Such performance is used in biomedical sensing, where slight differences in refractive index can help distinguish between normal and infected cells. Hence, the proposed absorber can serve as a promising refractive index-based biosensor for advanced sensing systems.

Table2. Various resonant frequencies (in THz) corresponding to the refractive index

Refractive Index	**Resonance frequency (in THz)**
1.31	3.2933
1.32	3.2907
1.33	3.2882
1.34	3.2857
1.35	3.2814
1.36	3.2810
1.37	3.278
1.38	3.2759
1.39	3.2734
1.40	3.2709



(a)



(b)

Fig.22 (a) Spectra of absorption for various refractive index **(b)** Linear fitting curve between resonant frequency and refractive index.

9.2 Simulation Results and Analysis for TB Detection:

In this study, the proposed sensor is utilized for the detection of different TB cells. The sensing mechanism is based on analyzing the variation in refractive index (RI) values between normal and infected cells. Here, the refractive index value of 1.351, corresponding to a normal cell as listed in table 3, is considered as the reference value for comparison during the detection process.

Table 3. The refractive index (RI) of normal and infected cell of TB

Cell name	Refractive index
TB1	Infected cell n_1=1.348 Normal cell n_2=1.351
TB2	Infected cell n_1=1.347 Normal cell n_2=1.351
TB3	Infected cell n_1=1.345 Normal cell n_2=1.351
TB4	Infected cell n_1=1.343 Normal cell n_2=1.351

Figure 23 illustrates the resonant absorption response of the proposed biosensor for different tuberculosis (TB) blood samples, namely TB1, TB2, TB3, and TB4. As shown in fig. 23(a) and Table 4, the resonance frequency obtained for the TB1 sample was 3.2835 THz, while the normal blood sample exhibited a slightly lower resonance frequency of 3.2814 THz. Similarly, for the TB2 sample, the observed resonance frequency increased to 3.2839 THz, resulting in a resonance frequency shift of 0.0025 THz, as presented in fig. 23(b) and table 4.

Fig. 23(c) and Fig. 23(d) show that the resonance frequencies of TB3 and TB4 are 3.2843 THz and 3.2852 THz, respectively. The resonance frequency shift is found to be 0.0029 THz for TB3 and 0.0038 THz for TB4. The plots in fig. 23 clearly states that the resonance absorption peaks corresponds to the infected samples (shown by the black curves) appear at higher frequencies compared to those of the healthy samples (shown by the red curves).

The blueshift observed in the results is mainly due to the changes in the effective electromagnetic properties of blood samples affected by TB. These changes occur because the refractive index of infected blood cells is different from that of healthy cells. As a result, the interaction between the incoming terahertz waves and the biosensor structure also changes.

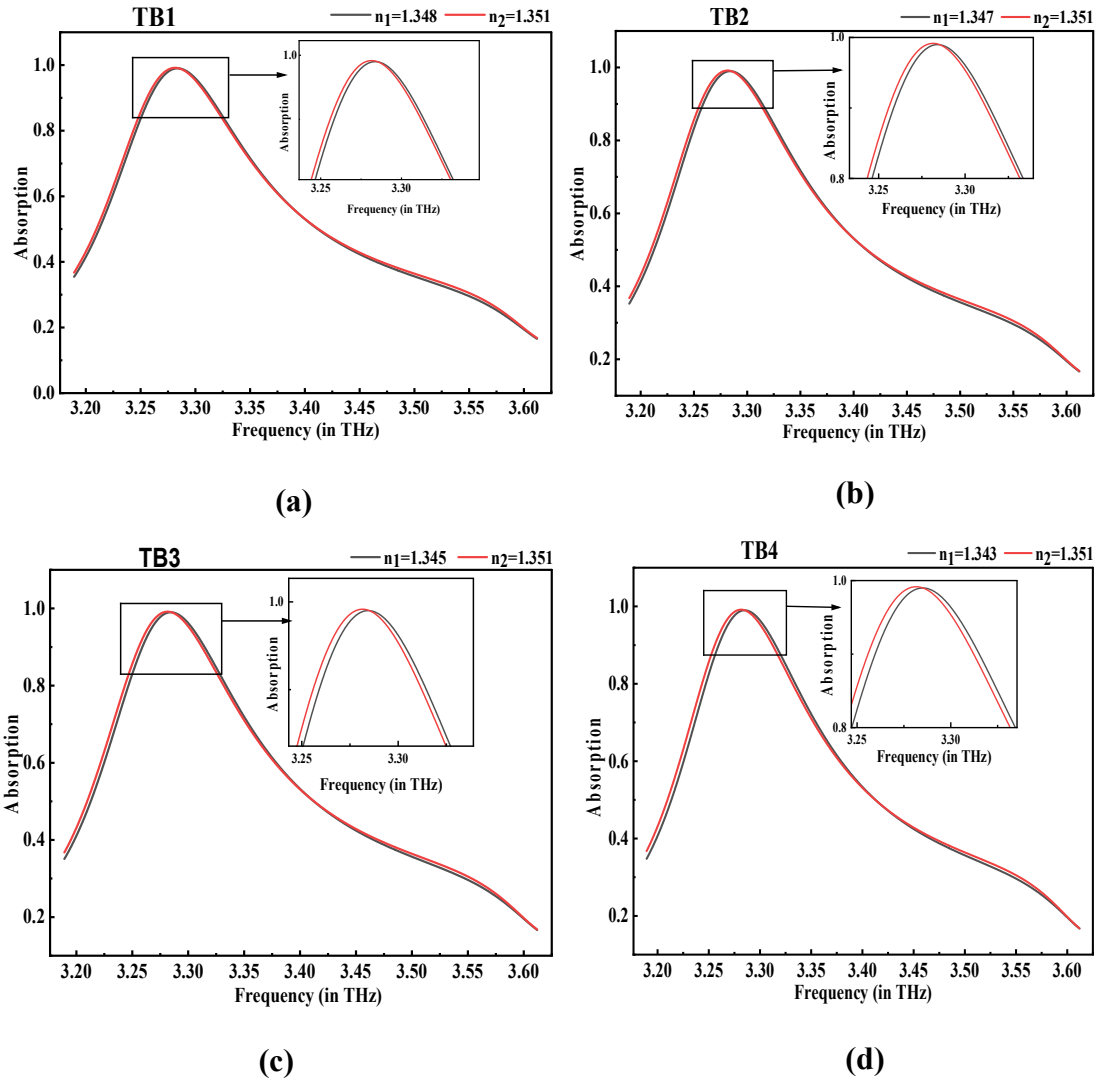


Fig.23 Absorption characteristics of the proposed biosensor for tuberculosis (TB) detection: **(a)** TB1 **(b)** TB2 **(c)** TB3 **(d)** TB4

The key sensing characteristics obtained for each TB sample are summarized in table 4. Among all four TB configurations, TB1 shows the best overall sensing performance. It achieves the highest sensitivity of 700 GHz/RIU along with a full width at half maximum (FWHM) of 0.2028 THz. A high figure of merit (FOM) of 3.4516 RIU^{-1}, and a Q-factor of 16.1908. These results indicate that TB1 provides good sensing capability as compared to TB2, TB3, and TB4.

Table 4 shows that TB2 gives a sensitivity of 625 GHz/RIU. Its FWHM is 0.2024 THz, while the FOM and Q factor are 3.0879 RIU^{-1} and 16.2248, respectively. TB3 shows a sensitivity of 483.3 GHz/RIU with an FWHM of 0.2020 THz. The obtained FOM is 2.3925 RIU^{-1} and the Q factor is 16.2589. For TB4, the sensitivity is 475 GHz/RIU, the FWHM is 0.2020 THz and its FOM is 2.3514 RIU^{-1}. Among all the samples, TB4 provides the highest Q factor of 16.2633 RIU^{-1}.

Table4. Performance of the proposed biosensor for Tuberculosis (Blood Sample) types corresponding normal cells

Cell name	**State**	**Refractive index (n)**	**Resonance frequency (THz)**	**Sensitivity (GHz/RIU)**	**FWHM (THz)**	**FOM (RIU^{-1})**	**Q-factor**
TB1	Normal	1.351	3.2814	700	0.2054	3.4079	15.9756
	Infected	1.348	3.2835		0.2028	3.4516	16.1908
TB2	Normal	1.351	3.2814	625	0.2054	3.0428	15.9756
	Infected	1.347	3.2839		0.2024	3.0879	16.2248
TB3	Normal	1.351	3.2814	483.3	0.2054	2.3529	15.9756
	Infected	1.345	3.2843		0.2020	2.3925	16.2589
TB4	Normal	1.351	3.2814	475	0.2054	2.3125	15.9756
	Infected	1.343	3.2852		0.2020	2.3514	16.2633

Table 5 shows a comparative analysis between the designed sensor and earlier published data related to this field. The comparison clearly shows that the designed metamaterial biosensor has offered improved sensing performance. And has achieves a sensitivity, of 700 GHz/RIU, outshining the other reported biosensors considered in this study.

Table5. Sensitivity comparison between our design and existing metamaterial biosensor

Reference	**Year**	**Absorption (%)**	**Sensitivity (GHz/RIU)**	**Sensing Application**
[35]	2025	96.9	666	Multi-Disease Detection TB
[47]	2025	96	374	Refractive index sensor
[42]	2025	98	583.3	Cervical cancer Detection
[48]	2025	---	400	Detection of COVID-19 Biomarkers
[49]	2024	----	153.85	Detection of multi-sclerosis
[50]	2023	---	504	Lung & Brain cancer
[37]	2022	---	207.14	Breast, Cervical cancer, Colorectal cancer
[51]	2022	---	325	Breast cancer detection
Proposed Work		99.88	700	TB Detection

CHAPTER 10

CONCLUSION

This thesis presents the design and analysis of a metamaterial based terahertz (THz) biosensor for sensing applications. The proposed sensor has a simple and effective structure which is made up of three closed ring resonators placed between two rectangular brick shaped structure. Vanadium dioxide (VO_2) was used to form the resonator layer. Paper was chosen as the dielectric substrate, while gold was used as the ground layer. These materials helped in achieving better electromagnetic behaviour along with strong absorption performance.

To achieve improved sensing performance, a detailed parametric study was done by changing the key structural parameters of the biosensor. The electric and magnetic field distributions were analyzed carefully to understand how terahertz electromagnetic waves interact with the metamaterial design. The analysis showed strong confinement of electromagnetic fields near the resonator regions. This strong field concentration played an important role in improving the absorption and sensing performance of the biosensor.

The optimized metamaterial sensor showed very high absorption performance, reaching a maximum absorptivity of 99.88% at a resonance frequency of 3.3777 THz in the frequency range of 3.2 to 3.6 THz. This strong absorption indicates proper impedance matching and an effective interaction between the incoming terahertz waves and the metamaterial design.

The proposed structure was also studied for terahertz biosensing applications using different TB analyte samples such as TB1, TB2, TB3, and TB4. The sensing behaviour was judged through various important parameters like sensitivity, quality factor, and figure of merit. The calculated sensitivities for TB1, TB2, TB3, and TB4 were 700 GHz/RIU, 625 GHz/RIU, 483.3 GHz/RIU, and 475 GHz/RIU, respectively. Among these

samples, TB1 showed the highest sensitivity of 700 GHz/RIU. It also provided a high figure of merit value of 3.4516 RIU^{-1}, which confirms the strong sensing ability of the designed biosensor. Also, TB4 produced the highest Q factor of 16.2633. This indicates a sharp resonance response and reliable sensing performance.

The results of this study show that the proposed metamaterial based THz biosensor has strong sensing and absorption performance. It provides high sensitivity, clear resonance characteristics, and excellent absorption efficiency. This design may also help future research related to the fabrication and practical use of THz metamaterial biosensors.

CHAPTER 11

FUTURE PERSPECTIVES

- Future research may also include broadband and multi-band metamaterial biosensors to do sensing in wider range.
- The proposed sensor can also be used for detecting the various other cells like viruses, glucose molecules, proteins, cancer cells.
- Artificial intelligence and machine learning-based optimization methods could be applied to simplify the design process and improve the overall performance of the biosensor.
- Development of flexible and wearable THz biosensors for portable biomedical applications.
- Efforts can also be made towards improving the environmental stability, fabrication simplicity.

CHAPTER 12

REFERENCES

1. Ramakrishna, S. Anantha, and Tomasz M. Grzegorczyk. *Physics and applications of negative refractive index materials*. CRC press, 2008.
2. Caloz, Christophe. "Perspectives on EM metamaterials." *Materials Today* 12, no. 3 (2009): 12-20.
3. Iyer, Ashwin K., and George V. Eleftheriades. "Negative refractive index metamaterials supporting 2-D waves." In *2002 IEEE MTT-S International Microwave Symposium Digest (Cat. No. 02CH37278)*, vol. 2, pp. 1067-1070. IEEE, 2002.
4. Caloz, Christophe, and Tatsuo Itoh. "Transmission line approach of left-handed (LH) materials and microstrip implementation of an artificial LH transmission line." *IEEE Transactions on Antennas and propagation* 52, no. 5 (2004): 1159-1166.
5. Khalil, Muhammad Amir, Wong Hin Yong, Md Shabiul Islam, Yew Chiong Lo, Ahasanul Hoque, Abdulmajeed M. Alenezi, Mohamed S. Soliman, and Mohammad Tariqul Islam. "Design and analysis of a quad-band perfect metamaterial absorber with enhanced sensing capabilities in the terahertz regime." *Physica Scripta* 100, no. 2 (2025): 025501.
6. Khodadadi, Bahareh, Majid Babaeinik, Vahid Ghods, and Pejman Rezaei. "Triple-band metamaterial perfect absorber for refractive index sensing in THz frequency." *Optical and Quantum Electronics* 55, no. 5 (2023): 431.
7. Jariwala, Deep, Artur R. Davoyan, Giulia Tagliabue, Michelle C. Sherrott, Joeson Wong, and Harry A. Atwater. "Near-unity absorption in van der Waals semiconductors for ultrathin optoelectronics." *Nano letters* 16, no. 9 (2016): 5482-5487.

8. Fountaine, Katherine T., Wen-Hui Cheng, Colton R. Bukowsky, and Harry A. Atwater. "Near-unity unselective absorption in sparse InP nanowire arrays." *ACS Photonics* 3, no. 10 (2016): 1826-1832.
9. Khalil, Muhammad Amir, Wong Hin Yong, Ahasanul Hoque, Md Shabiul Islam, Lo Yew Chiong, Cham Chin Leei, Ahmed Alzamil, and Mohammad Tariqul Islam. "A compact quad-square negative-index metamaterial: Design, simulation, and experimental validation for microwave applications." *APL Materials* 12, no. 6 (2024).
10. Fei, Peng, Guy AE Vandenbosch, Weihua Guo, Xin Wen, Di Xiong, Wei Hu, Qi Zheng, and Xing Chen. "Versatile cross-polarization conversion chiral metasurface for linear and circular polarizations." *Advanced Optical Materials* 8, no. 13 (2020): 2000194.
11. Teng, Shuyun, Qi Zhang, Han Wang, Lixia Liu, and Haoran Lv. "Conversion between polarization states based on a metasurface." *Photonics Research* 7, no. 3 (2019): 246-250.
12. Pawar, Ashish Y., Deepak D. Sonawane, Kiran B. Erande, and Deelip V. Derle. "Terahertz technology and its applications." *Drug invention today* 5, no. 2 (2013): 157-163.
13. Chen, Xu, and Wenhui Fan. "Ultrasensitive terahertz metamaterial sensor based on spoof surface plasmon." *Scientific reports* 7, no. 1 (2017): 2092.
14. Grigorenko, A. N., A. K. Geim, H. F. Gleeson, Ying Zhang, A. A. Firsov, I. Y. Khrushchev, and J. Petrovic. "Nanofabricated media with negative permeability at visible frequencies." *Nature* 438, no. 7066 (2005): 335-338.
15. Schurig, D. R. S. D., J. J. Mock, and D. R. Smith. "Electric-field-coupled resonators for negative permittivity metamaterials." *Applied physics letters* 88, no. 4 (2006).
16. Pendry, John B., Anthony J. Holden, David J. Robbins, and William J. Stewart. "Magnetism from conductors and enhanced nonlinear phenomena." *IEEE transactions on microwave theory and techniques* 47, no. 11 (1999): 2075-2084.

17. Landy, Nathan I., Soji Sajuyigbe, Jack J. Mock, David R. Smith, and Willie J. Padilla. "Perfect metamaterial absorber." *Physical review letters* 100, no. 20 (2008): 207402.

18. Engheta, Nader. "Thin absorbing screens using metamaterial surfaces." In *IEEE Antennas and Propagation Society International Symposium (IEEE Cat. No. 02CH37313)*, vol. 2, pp. 392-395. IEEE, 2002.

19. Qin, Gang, Jia-Fu Wang, Ming-Bao Yan, Wei Chen, Hong-Ya Chen, and Yong-Feng Li. "Lowering plasma frequency by enhancing the effective mass of electrons: A route to deep sub-wavelength metamaterials." *Chinese Physics B* 22, no. 8 (2013): 087302.

20. Hao, Jiaming, Lei Zhou, and Min Qiu. "Nearly total absorption of light and heat generation by plasmonic metamaterials." *Physical Review B—Condensed Matter and Materials Physics* 83, no. 16 (2011): 165107.

21. Soukoulis, Costas M., Stefan Linden, and Martin Wegener. "Negative refractive index at optical wavelengths." *Science* 315, no. 5808 (2007): 47-49.

22. Al-Adhami, Ammar, Yasir Al-Adhami, and Taha A. Elwi. "A 3D antenna array based solar cell integration for modern MIMO systems." *Infocommunications Journal* 15, no. 4 (2023): 10-16.

23. Ismail, Marwa M., Taha A. Elwi, and Ali J. Salim. "Reconfigurable composite right/left-handed transmission line antenna based Hilbert/Minkowski stepped impedance resonator for wireless applications." *Radioelectronic and Computer Systems* 1 (2023): 77-91.

24. Jassim, Yaser Amer, Mesut Çevik, and Taha A. Elwi. "10ghz printed circuit antenna for wireless power transfer applications." In *2023 5th International Congress on Human-Computer Interaction, Optimization and Robotic Applications (HORA)*, pp. 1-4. IEEE, 2023.

25. Alibakhshikenari, Mohammad, Bal S. Virdee, Ayman A. Althuwayb, Dion Mariyanayagam, and Ernesto Limiti. "Compact and low-profile on-chip antenna

using underside electromagnetic coupling mechanism for terahertz front-end transceivers." *Electronics* 10, no. 11 (2021): 1264.

26. Althuwayb, Ayman A., Mohammad Alibakhshikenari, Bal S. Virdee, Harry Benetatos, Francisco Falcone, and Ernesto Limiti. "Antenna on chip (AoC) design using metasurface and SIW technologies for THz wireless applications." *Electronics* 10, no. 9 (2021): 1120.
27. Alibakhshikenari, Mohammad, Bal S. Virdee, Mohsen Khalily, Chan H. See, Raed Abd-Alhameed, Francisco Falcone, Tayeb A. Denidni, and Ernesto Limiti. "High-gain on-chip antenna design on silicon layer with aperture excitation for terahertz applications." *IEEE Antennas and Wireless Propagation Letters* 19, no. 9 (2020): 1576-1580.
28. Khalil, Muhammad Amir, Wong Hin Yong, Mohammad Tariqul Islam, Ahasanul Hoque, Md Shabiul Islam, Cham Chin Leei, and Mohamed S. Soliman. "RETRACTED ARTICLE: Double-negative metamaterial square enclosed QSSR For microwave sensing application in S-band with high sensitivity and Q-factor." *Scientific Reports* 13, no. 1 (2023): 7373.
29. Alibakhshikenari, Mohammad, Bal S. Virdee, Panchamkumar Shukla, Naser Ojaroudi Parchin, Leyre Azpilicueta, Chan Hwang See, Raed A. Abd-Alhameed et al. "Metamaterial-inspired antenna array for application in microwave breast imaging systems for tumor detection." *IEEE Access* 8 (2020): 174667-174678.
30. Rabbani, Md Golam, Mohammad Tariqul Islam, Ahasanul Hoque, Badariah Bais, Saleh Albadran, Md Shabiul Islam, and Mohamed S. Soliman. "Orthogonal centre ring field optimization triple-band metamaterial absorber with sensing application." *Engineering Science and Technology, an International Journal* 49 (2024): 101588.
31. khalil, Muhammad Amir, Wong Hin Yong, Mohammad Tariqul Islam, Ahasanul Hoque, Md Rashedul Islam, and Md Shabiul Islam. "A perfect metamaterial absorber for sensing application of edible oil." In *International Conference on*

Space Science and Communication, pp. 357-364. Singapore: Springer Nature Singapore, 2023.

32. Almizan, Hayder, Marwah Haleem Jwair, Yahiea Al Naiemy, Zaid A. Abdul Hassain, Lajos Nagy, and Taha A. Elwi. "Novel metasurface based microstrip antenna design for gain enhancement RF harvesting." *Infocommunications Journal* 15, no. 1 (2023): 2-8.
33. Ullah, Najeeb, Md Shabiul Islam, Ahasanul Hoque, Wong Hin Yong, Mohamed S. Soliman, Saleh Albadran, and Mohammad Tariqul Islam. "A compact complementary split ring resonator (CSRR) based perfect metamaterial absorber for energy harvesting applications." *Engineering Science and Technology, an International Journal* 45 (2023): 101473.
34. Ragavan, VK Senthil, N. S. Nithya, Anantharamaiah Vengala, Balambigai Subramanian, and C. Ambhika. "Refractive Index Biosensor–Based Detection of Mycobacterium Tuberculosis Using Sea Lion Political Optimizer and Deep Learning." *Plasmonics* 20, no. 10 (2025): 9247-9265.
35. Singh, Neelam, Reshmi Dhara, and Sanoj Mahato. "Terahertz-based biosensing technology for multi-disease detection: Cancer, malaria, bacillus virus, and tuberculosis diagnosis." *Optik* 332 (2025): 172323.
36. Saadeldin, A. Samy, Mohamed Farhat O. Hameed, Essam MA Elkaramany, and Salah SA Obayya. "Highly sensitive terahertz metamaterial sensor." *IEEE Sensors Journal* 19, no. 18 (2019): 7993-7999.
37. Patel, Shobhit K., Jaymit Surve, and Juveriya Parmar. "Detection of cancer with graphene metasurface-based highly efficient sensors." *Diamond and Related Materials* 129 (2022): 109367.
38. Guo, Wenjing, LiHong Zhai, Zeinhom M. El-Bahy, Zhumao Lu, Lu Li, Ashraf Y. Elnaggar, Mohamed M. Ibrahim, Huiliang Cao, Jing Lin, and Bin Wang. "Terahertz metamaterial biosensor based on open square ring." *Advanced Composites and Hybrid Materials* 6, no. 3 (2023): 92.

39. Qu, Zeng, Jinfeng Kang, Wei Li, Boyi Yao, Hao Deng, Yiqing Wei, Huihui Jing, Xiaohong Li, Junping Duan, and Binzhen Zhang. "Microstructure-based high-quality factor terahertz metamaterial bio-detection sensor." *Advanced Composites and Hybrid Materials* 6, no. 3 (2023): 100.
40. Zhang, Huo, Chengfeng Liu, Chuanpei Xu, Zhi Li, Yuee Wang, and Yifu Peng. "A dual-band terahertz metamaterial sensor with high Q-factor and sensitivity." *Optical & Quantum Electronics* 55, no. 13 (2023).
41. Aliouar, Tahar, Fatima Djerfaf, Djalal eddine Bensafieddine, and Fathi Bendelala. "A new performed metamaterial biosensor for the early detection of cancer cells." *Plasmonics* 20, no. 9 (2025): 7611-7618.
42. Tammam, Mahmoud Maree E., Mohamed Farhat O. Hameed, Essam MA Elkaramany, Tamer A. Ali, and S. S. A. Obayya. "Versatile terahertz metamaterial sensor for biomedical applications." *Plasmonics* 20, no. 5 (2025): 2815-2828.
43. Zhang, Jin, Ning Mu, Longhai Liu, Jianhua Xie, Hua Feng, Jianquan Yao, Tunan Chen, and Weiren Zhu. "Highly sensitive detection of malignant glioma cells using metamaterial-inspired THz biosensor based on electromagnetically induced transparency." *Biosensors and Bioelectronics* 185 (2021): 113241.
44. Luo, Hao, Hai Liu, Cong Chen, Yue Feng, Peng Gao, Zi Yan Ren, and Yu Jia Qiao. "Dual-broadband terahertz absorber based on phase transition characteristics of VO2." *Results in Physics* 34 (2022): 105270.
45. Mohammed, Mustafa M., Halgurd N. Awl, Zhwan M. Rashid, Rashad H. Mahmud, and Yadgar I. Abdulkarim. "Simulated study of a broadband terahertz metamaterial absorber based on vanadium dioxide resonator for cancer detection applications." *Plasmonics* 20, no. 10 (2025): 9225-9236.
46. Banerjee, Sagnik, Purba Dutta, Amitkumar Vidyakant Jha, Bhargav Appasani, and Mohammad S. Khan. "A biomedical sensor for detection of cancer cells based on terahertz metamaterial absorber." *IEEE Sensors Letters* 6, no. 6 (2022): 1-4.

47. Mahfuz, Tasnim, Arif Hossan, and Naymur Rahman. "Design of a polarization independent terahertz metamaterial absorber for biomedical sensing applications." *Biosensors and Bioelectronics: X* 22 (2025): 100560.
48. Wekalao, Jacob, and Shobhit K. Patel. "Design and analysis of a plasmonic metasurface-based graphene sensor for highly sensitive and label-free detection of COVID-19 biomarkers." *Plasmonics* 20, no. 4 (2025): 2109-2121.
49. Alsalman, Osamah, Jacob Wekalao, U. Arun Kumar, Dhruvik Agravat, Juveriya Parmar, and Shobhit K. Patel. "Design of split ring resonator graphene metasurface sensor for efficient detection of brain tumor." *Plasmonics* 19, no. 1 (2024): 523-532.
50. Wang, Peiliang, Jing Lou, Yun Yu, Lang Sun, Lan Sun, Guangyou Fang, and Chao Chang. "An ultra-sensitive metasurface biosensor for instant cancer detection based on terahertz spectra." *Nano Research* 16, no. 5 (2023): 7304-7311.
51. Fang, Weihao, Zhengtai Ma, Xiaoqing Lv, Jian Liu, Weihua Pei, and Zhaoxin Geng. "Flexible terahertz metamaterial biosensor for label-free sensing of serum tumor marker modified on a non-metal area." *Optics Express* 30, no. 10 (2022): 16630-16643.

Ajeet KUMAR

Barbie_Thesis_Plag_check

BTECH

Document Details

Submission ID
trn:oid:::27535:140632527

Submission Date
May 27, 2026, 1:23 PM GMT+5:30

Download Date
May 27, 2026, 1:26 PM GMT+5:30

File Name
Barbie_Thesis_Plag_check.pdf

File Size
1.4 MB

50 Pages

9,586 Words

53,610 Characters

5% Overall Similarity

The combined total of all matches, including overlapping sources, for each database.

Filtered from the Report

- Bibliography
- Small Matches (less than 12 words)

Match Groups

33 Not Cited or Quoted 5%
Matches with neither in-text citation nor quotation marks

0 Missing Quotations 0%
Matches that are still very similar to source material

0 Missing Citation 0%
Matches that have quotation marks, but no in-text citation

0 Cited and Quoted 0%
Matches with in-text citation present, but no quotation marks

Top Sources

3% Internet sources
3% Publications
2% Submitted works (Student Papers)

Integrity Flags

0 Integrity Flags for Review

Our system's algorithms look deeply at a document for any inconsistencies that would set it apart from a normal submission. If we notice something strange, we flag it for you to review.

A Flag is not necessarily an indicator of a problem. However, we'd recommend you focus your attention there for further review.

Ajeet KUMAR

Barbie_Thesis_Plag_check

BTECH

Document Details

Submission ID
trn:oid:::27535:140632527

Submission Date
May 27, 2026, 1:23 PM GMT+5:30

Download Date
May 27, 2026, 1:27 PM GMT+5:30

File Name
Barbie_Thesis_Plag_check.pdf

File Size
1.4 MB

50 Pages

9,586 Words

53,610 Characters

*% detected as AI

AI detection includes the possibility of false positives. Although some text in this submission is likely AI generated, scores below the 20% threshold are not surfaced because they have a higher likelihood of false positives.

Caution: Review required.

It is essential to understand the limitations of AI detection before making decisions about a student's work. We encourage you to learn more about Turnitin's AI detection capabilities before using the tool.

Disclaimer

Our AI writing assessment is designed to help educators identify text that might be prepared by a generative AI tool. Our AI writing assessment may not always be accurate (i.e., our AI models may produce either false positive results or false negative results), so it should not be used as the sole basis for adverse actions against a student. It takes further scrutiny and human judgment in conjunction with an organization's application of its specific academic policies to determine whether any academic misconduct has occurred.